SwissFEL

ESB-MX instrument for fixed target protein crystallography at SwissFEL:
Concept design report

Status: 29.09.2016 (V2)

PAUL SCHERRER INSTITUT
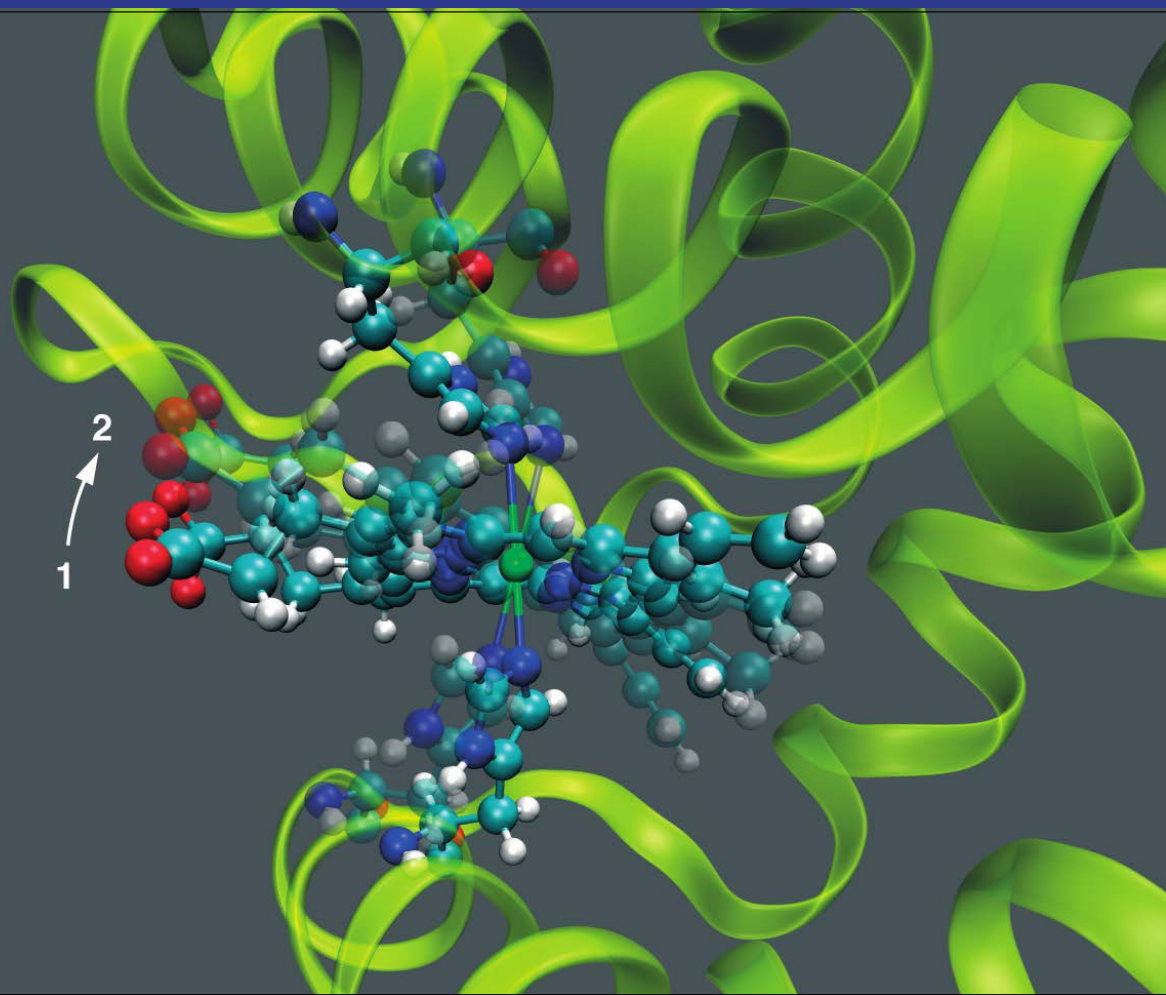
ESB-MX instrument for fixed target protein crystallography at SwissFEL: Concept Design Report

Bill Pedrini, Isabelle Martiel, Ezequiel Panepucci, Claude Pradervand

Version 2, 29.09.2016

The goal of the ESB-MX project is to build an instrument dedicated to fixed-target protein crystallography at the Swiss x-ray free electron laser (SwissFEL), ready for commissioning in Spring 2018. This Concept Design Report (CDR) describes the most relevant features of the ESB-MX instrument, the basic concepts guiding its design, and the aspects related to the integration in the SwissFEL experimental station infrastructure.

The measurements will be possible for photon energies above 5.0 keV, either in air or in helium atmosphere, and at either room or cryogenic temperatures. Diffraction data can be collected serially at up to 100 Hz on preparations of many small crystals (< 5 μm) by scanning the sample support, or at lower rate by means of helical scans on larger crystals. The instrument is conceived as a movable, standalone unit, suitable to be employed at the SwissFEL Experimental Station B (ESB) in the early years, and at other future hard X-ray SwissFEL stations later on.

PAUL SCHERRER INSTITUT

Content list

List of Figures

List of Tables

1 Introduction

1.1 Motivations and possibilities of protein crystallography at X-FELs

X-ray Free Electron Lasers (XFELs) are currently pushing the limits of protein X-ray crystallography (PX) for atomic-resolution structure determination of macromolecules beyond the possibilities offered at third generation synchrotron sources [1]. The "diffract-before-destroy" approach [2, 3] relies on the extremely short and intense XFEL pulses, of less than 50 fs duration and up to few mJ energy, and leads to radiation damage-free protein structures. Therefore, XFELs have the potential to enable high-resolution structure determination on more challenging protein targets. These can be membrane proteins, metalloproteins and proteins with disulfide bridges, all prone to beam damage, as well as proteins that form only small crystals, which again is typical for membrane proteins. Recent results suggest that the crystals smaller than few micrometers cannot be studied at synchrotron sources using the currently standard methods of measuring one or few crystals in air [4]. In parallel, the dynamic functional study of biological macromolecules in the crystalline matrix at femto- to picosecond time-resolution becomes possible at XFELs. The relevance of XFEL based protein structure investigations is reflected in the large amount of beam time allocated at the currently operational XFEL facilities.

The injection of nano- and micrometer-sized crystals suspended in a liquid or in a viscous medium has been the first and therefore historically privileged sample delivery method for PX at XFELs [3, 5-8]. It indeed enables in a straightforward manner to reach frame acquisition albeit not hit rates of the order of 100 Hz, thus matching the repetition rate of most of the XFEL sources currently in operation or realization. More recently, the alternative method of fixed-target sample delivery has emerged. Fixed-target means that the protein crystals are fixed on a solid support whose position in the beam is controlled by the user. Two different data collection approaches have been pursued: (i) serial data acquisition by scanning a solid support carrying a multitude of small protein crystals [9], and (ii) synchrotron-like data acquisition with rotations on larger crystals [10, 11]. After first demonstrations, fixed target methods have rapidly attracted the interest of a more enlarged PX community, and are now developing rapidly to a major alternative to injection methods. Indeed, fixed target methods cover almost all scientific cases that justify allocation of expensive XFEL beamtime, keep up with the repetition rates of current XFEL facilities that provide hard X-rays, and exhibit a number of operational advantages:

1. Cryogenic cooling of the crystal during X-ray data collection becomes possible, which will be the approach of choice for precious samples available in minute quantities, and for which physiological temperatures are not strictly required. Following a well-established procedure for synchrotron measurements, the crystals can be frozen in their optimal development state ahead of beamtime, which also guarantees preservation during the transport to the X-ray facility.

2. The sample consumption is drastically reduced with respect to injection-based measurements [9].

3. Fragile crystals are not subject to damage by high pressures, shear forces or electric charging during the injection process.

4. For larger crystals, control of the crystal orientation and diagnostics of the crystal prior to the destruction by the X-ray pulse becomes possible.

5. A number of practical issues of the injection method are avoided, such as the frequently observed clogging of the injection device itself [12].

The fixed-target concept encompasses a number of different supports. These include silicon nitride membranes [9, 13], silicon chips [14], polymer and TEM-compatible mounts [15], microfluidic devices [12], plastic grids and micromesh mounts [10], and standard protein crystallography pins for large crystals [11] or microcrystal slurries [16]. Currently, the technical development are directed towards the following goals: (i) improving the crystal hit rate for scanning serial data acquisition on microcrystal preparations, and consequently decreasing the sample consumption and optimizing the use of the beam [13]; this may be possible either by pre-positioning the crystals on the support [12] or by pre-locating them using imaging techniques such as UV microscopy [17] or second order nonlinear imaging of chiral crystals (SONICC)[1]; (ii) developing sample preparation protocols for non-cryogenic measurements, which ensure sample preservation during data acquisition [13, 15]; (iii) reducing the X-ray background caused by the supporting material; and (iv) promoting compatibility of sample support technologies with other investigation tools (cryo electron microscopy, mass spectrometry).

1.2   Worldwide protein crystallography possibilities at XFELs

The XFEL facilities which are now operational or under construction are listed in Table 1, along with the X-ray parameters most relevant for the protein crystallography experiments. As pointed out in the following, all facilities put a strong emphasis on femtosecond protein crystallography.

At the Linac Coherent Light Source (LCLS) [18] in Stanford, USA, the portion of user beamtime allocated to protein crystallography has increased up to about 25% (March – August 2016 LCLS schedule).   Currently, jet experiments with Gas Dynamic Virtual Nozzle (GDVN), Lipidic Cubic Phase (LCP) and concentric-flow microfluidic electrokinetic sample holder (coMESH) [19] are conducted routinely in the vacuum chamber of the CXI (Coherent Diffraction Imaging) station [20], while fixed target experiments are performed at the XPP (X-ray Pump and Probe) station using custom scanning setups [14, 21] or the setup adapted from the SSRL synchrotron [10]. Moreover, the new MFX (Macromolecular Femtosecond Crystallography) station [22] is permanently dedicated to protein crystallography, replacing the setup previously in operation at the XPP station, and can be operated in parallel with XPP. For fixed-target experiments, the MFX instrumentation includes a goniometer, with a version capable of 120 Hz frame acquisition rate in development, and a cryogenic stream. This equipment can be removed to install a stand for a sample injector for jet experiments, or custom setups provided by users.

The LCLS-II upgrade [23] is foreseen to be completed in 2020, which results in longer facility shutdowns in the period 2017 – 2020. The upgrade includes a new, additional superconducting accelerator which, for photon energies below 5 keV, will enable X-ray pulse rates above 1 kHz with pulse energies up to 1 mJ at 1 keV and 0.02 mJ at 5 keV. This may be exploited for liquid-jet based PX experiments at a higher repetition rate and a lower photon energy, provided that the reduced pulse energy is not an obstacle. The present 120 Hz room-temperature LCLS accelerator won't be subject of major upgrades, thus leaving the present fixed-target PX capabilities and developments unaffected.

At the SACLA XFEL facility [24] in Harima, Japan, 14 % of the total beamtime was allocated to protein crystallography in 2014, with increasing trend. Various setups are available for both jet- and fixed-target-based experiments, which can be installed either at the BL2 or BL3 stations [25]. Injectors have been developed for liquid and viscous carrier media. The DAPHINIS setup

[26] offers a helium environment for jet-based experiments. Fixed-target scanning experiments can be carried out in the MAXIC vacuum chamber [27], however this setup is mainly used for single particle imaging at present. A synchrotron-like setup is periodically installed for damage-free structural studies on large crystals [11].

The European XFEL (EuXFEL) [28] in Hamburg, Germany, is foreseen to host first users by the end of 2017. The burst-mode X-ray pulse structure and the resulting high average repetition rate appear favorable to jet-based protein crystallography experiments, planned at the SPB/SFX instrument [29]. Fixed-target experiments at the low repetition rate of 10 Hz are foreseen at the SPB instrument [29, 30] and at the FXE instrument [31, 32], which may accommodate a scanning setup of similar design as the one developed at Diamond Light Source [21].

The Pohang Accelerator Laboratory XFEL (PAL FEL) [33] in Pohang, Korea, is foreseen to start operation in 2017. The HES2 station will host femtosecond crystallography and coherent X-ray imaging experiments. More precise information regarding protein crystallography instrumentation plans is not available. Nevertheless, transfer of technological knowledge resulting from experiences at other XFEL facilities is expected.

The Swiss Free Electron Laser (SwissFEL) ([34]) at the Paul Scherrer Institute in Villigen, Switzerland, is foreseen to start operation in 2017. More details on the facility and the protein crystallography possibilities are given in Section 1.3.

In summary, jet- and fixed-target-based delivery possibilities for protein crystallography are currently provided or foreseen at different levels in all XFEL facilities. It is likely that fast, low-viscosity jet delivery may become more attractive at high repetition rate facilities European XFEL and LCLS-II. In contrast, fixed-target methods do not profit significantly from the increased rate. Consequently, the present demand for XFEL fixed-target protein crystallography experiments especially at sources with repetition rates in the 100 Hz range is expected to persist in the future.

FEL, Institution	Location	Start of operation	Repetition rate	Photon energy	Rel. bandwidth	Pulse length	Pulse energy
			Hz	keV	%	fs (FWHM)	mJ
LCLS, SLAC	Palo Alto, CA, USA	2009	120	4.0 – 10.0	0.1	10 – 300	0.2 – 3
SACLA, RIKEN	Harima, J	2012	30 (60)	4.9 – 15.0	0.5	< 10	< 0.3
PAL-FEL	Pohang, KOR	2016	60	5.0 – 12.0	0.2	< 100	< 2
SwissFEL, PSI	Villigen, CH	2017	100	2.0 – 12.4	0.2	5 - 50	0.2 – 1.4
EuXFEL, DESY	Hamburg, D	2017	10 x 2700	3.0 – 25.0	0.1	2 - 100	0.06 - 2

Table 1. Worldwide hard X-ray XFEL facilities.

List of XFEL facilities worldwide that provide hard X-ray radiation of energy above 5 keV. The most relevant X-ray pulse parameters in Self Amplified Spontaneous Emission operation mode are given. The values are taken from the webpages describing the instruments and from [24, 25, 33, 35].

1.3   The SwissFEL project

1.3.1   Overview

The scientific case for the Swiss Free Electron Laser (SwissFEL) dates back to 2010, and is available at the SwissFEL homepage [36]. The current design (Figure 1) includes a hard X-ray beamline, named ARAMIS, which will be commissioned in 2017, and a soft X-ray beamline,

named ATHOS, which is expected to be realized by 2020. The two beamlines can be operated simultaneously at 100 Hz, with two electron bunches exploiting the same initial accelerator section and separated by 28 ns in time.
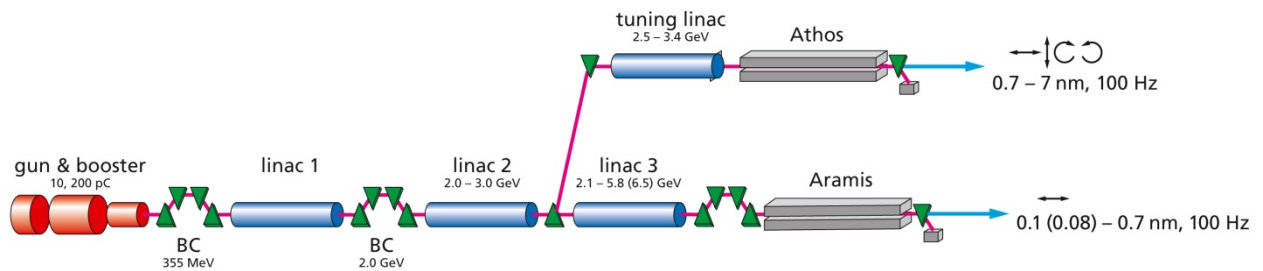
Figure 1. SwissFEL overall layout.

The graphics shows the layout of the SwissFEL accelerator and undulator layout, which includes the hard X-ray line ARAMIS and the soft X-ray beamline ATHOS.

1.3.2 The hard X-ray beamline ARAMIS

The hard X-ray beamline ARAMIS (CDR available at the SwissFEL homepage [36]) is designed for photon energies in the range 2.0 – 12.4 keV. With a possible future accelerator upgrade, the upper limit may be shifted to 14.4 keV. In the standard SASE operation mode, the duration of the photon pulses will be 2 – 21 fs RMS (5 - 50 fs FWHM), the relative bandwidth will be of the order of $2 \cdot 10^{-3}$, and the pulse energy for the long pulse mode is predicted to be about 1.4 mJ from start-to-end simulations.

The layout of the experimental stations is shown in Figure 2. A system of offset mirrors, placed in the optical hutch, directs the X-ray beam along three different beamline branches, named ARAMIS-1 to ARAMIS-3, to either one of the three subsequent experimental hutches downstream. The first two hutches will host the Experimental Stations ESA and ESB, which are expected to host first pilot users in fall 2017. A third branch with an Experimental Station of name ESC, located in the third hutch, is currently in the conception phase and will be realized later. Each experimental station will be served by a pump-laser to perform time-resolved experiments.
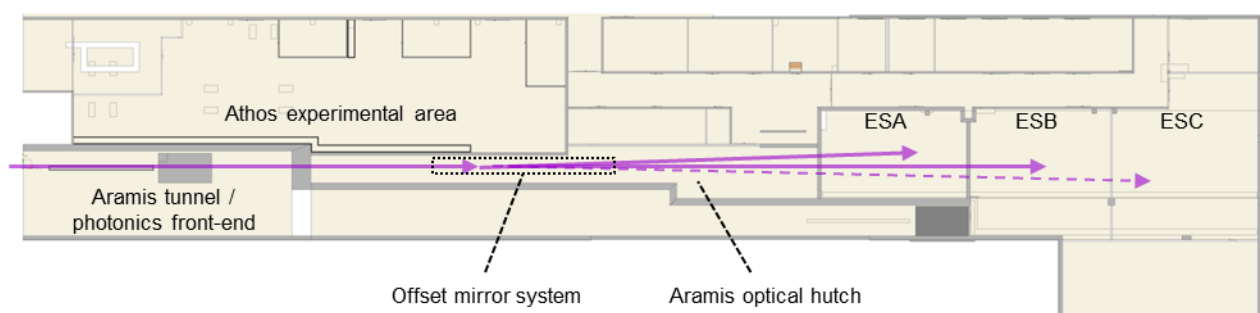
Figure 2. ARAMIS layout.

Top-view of the ARAMIS beamline area. The X-ray beam path is represented by magenta arrows, and can be directed to either of the three experimental hutches by a system of retractable plane offset mirrors positioned in the optical hutch. The extension of the experimental area in each hutch is about 14 x 10 m.

1.3.3 The ARAMIS experimental stations

The first ARAMIS experimental station ESA (CDR available at the SwissFEL homepage [36]) is dedicated to time-resolved X-ray spectroscopy and scattering for chemical investigations, and to

serial femtosecond protein crystallography. The station consists of two setups, called ESA-PRIME and ESA-FLEX, installed permanently at two different sample positions along the X-ray beam. ESA-PRIME consists of an experimental chamber which integrates a 16M Jungfrau pixel detector in the forward direction, and a van Hamos emission spectrometer with crystals and Jungfrau detector modules in a separate compartment lateral to the beam. The beam can be focused to 1.5 µm (FWHM). The sample can be maintained not only in air or nitrogen, but also in vacuum or helium. Thus, also the lower energies of the full range 2.0 – 12.4 keV can be covered. ESA-FLEX is a flexible instrument for in-air measurements, where the beam size can be set to 10 µm (FWHM) or larger. It is equipped with a variable configuration van Hamos emission spectrometer, but can also accommodate other custom user setups.

The second ARAMIS experimental station ESB (CDR available at the SwissFEL homepage [36]) is dedicated to time-resolved resonant and non-resonant X-ray diffraction in condensed matter physics investigations. The station is characterized by a single sample position, at which the X-ray beam with energies in the range 4.5 – 12.4 keV can be focused down to 2 µm (FWHM), or defocused up to 200 µm (FWHM). The experiments can be performed on two different platforms. The ESB-XRD platform is a diffractometer with a 1M Jungfrau detector mounted on the diffractometer arm. The ESB-GPS platform is a heavy load manipulator which can accommodate custom user equipment. Either one of the two setups can be moved to the sample position on rails fixed to the floor in direction perpendicular to the beam. A 16M Jungfrau pixel detector will be mounted on a robot arm attached on the ceiling of the hutch, and can be placed at any position reached by the arm.

1.3.4   The Jungfrau pixel detector technology at SwissFEL

For pixel array detectors in the hard X-ray regime, the SwissFEL project relies on the Jungfrau technology, developed at PSI explicitly for FEL applications. The detection principle relies on charge integration but with single photon counting capabilities. The square shaped pixels have size of 72 µm. The technology is modular, such that the 0.5M modules of 8 x 4 cm size can be assembled in a flexible manner to cover larger areas. More technical features are reported in section 7.1.

1.4   Protein crystallography possibilities at SwissFEL

1.4.1   Jet-based experiments at ESA-PRIME

The requirements for jet-based protein crystallography experiments have been taken into account in the design of the ESA-PRIME instrument. Photon energy range, beam size and sample atmosphere (Section 1.3.3) are suitable. The chamber is designed to host injectors delivering the protein crystals within a liquid or viscous jet [1]. The diffraction images will be recorded with the 16M Jungfrau detector. Simultaneous acquisition of single-shot X-ray emission spectra will be possible with the installed van Hamos spectrometer.

1.4.2   The ESB-MX project for fixed-target experiments

The original concept for the SwissFEL ARAMIS experimental stations did not include instrumentation designed specifically for fixed-target protein crystallography. A general purpose sample positioning stage will be available in the chamber of the ESA-PRIME station. However, the limited speed and positioning accuracy of the stage, the lack of a motorized rotation axis, and the physical obstacles to frequent sample exchange represent severe limitations to efficient and high-throughput fixed-target data collection.

The promising results from fixed-target protein crystallography experiments at XFELs reported in 2014 [9-11, 13] and the conclusions drawn from a workshop held at PSI in January 2015 have triggered the SwissFEL management, in agreement with the Macromolecular Crystallography (MX) group of the Swiss Light Source (SLS), to initiate the effort to offer the fixed-target approach as a standard method at SwissFEL. Several possibilities were considered, but it soon became clear that beam parameters and infrastructure foreseen at the ESB station are best suited to the scope. Thus, in March 2015 the ESB-MX project was initiated, with the goal of building an instrument dedicated fully to fixed-target protein crystallography that is ready for commissioning in 2018. The instrument will be installed at the ESB station for measurement campaigns of 5 – 6 days. Because it is easily mountable and dismountable, the instrument is also suited for operation at the future experimental station ESC.

Fixed-target protein crystallography has been thoroughly developed during the last decades at synchrotron X-ray sources, and the application to XFELs only requires some adaptation of sample handling and data collection methods. The ESB-MX project is a joint collaboration between SwissFEL and SLS-MX group, which unifies the PSI efforts towards further development of fixed-target serial crystallography methods at both the SLS protein crystallography (PX) beamlines and SwissFEL. Moreover, key positions in the project organization are occupied by members of the SLS-MX group, which ensures effective implementation of the knowledge available at PSI into the ESB-MX instrument. From a strategical point of view, the realization of the instrument will allow to build-up expertise in fixed-target methods on site, which is impossible otherwise. With the present schedule, this will be possible almost from the start of SwissFEL operation.

1.4.3   The ESB-MX project Concept Design Report

The present document is the Concept Design Report (CDR) of the ESB-MX instrument, and aims to describe the project goals, the features of the instruments, and how the crucial technical challenges are going to be solved. Sections 2 and 3 are on higher conceptual level, and are addressed to a general user. Section 4 describes the layout of the instrument. Section 5 is written almost as a Technical Design report, and addresses in some detail specific technical issues that were considered relevant already at the present stage of the project.

2   ESB-MX project objectives

The objective of the ESB-MX project is to realize an instrument for fixed-target protein crystallography with the following features:

- The instrument is suitable for <u>operation at the ESB</u> experimental station of SwissFEL

- The instrument is <u>movable</u>: it can be installed or removed within 12 hours

- The instrument can operate at photon energies in the range <u>5.0 – 12.7 keV</u>, achieving better than <u>1 Å resolution</u> with 12.4 keV radiation

- The instrument is equipped with an <u>automated sample changer</u>, with sample exchange time shorter than 20 s

- The instrument allows the measurements to be performed both in <u>air or helium atmosphere</u>

- The instrument allows to measure samples at both at <u>room temperature or cryogenic conditions</u> for both air or helium atmospheres

- The instrument permits <u>100 Hz serial scanning data collection</u> on samples consisting of a large number of small crystals (< 5 μm) positioned in regular or irregular pattern on a chip

- The instrument permits <u>synchrotron-like data collection</u> on large crystals by combined translations and rotations to collect diffraction data from a same crystal at different positions and in different orientations

- The instrument can be <u>upgraded to permit laser-pump / X-ray probe experiments</u>

3   ESB-MX instrument key concepts

The concepts judged to be most relevant from the perspective of the users of the ESB-MX instrument are summarized in this section. The instrument is designed to be dedicated fully to fixed target protein crystallography. However, measurements related to other scientific areas can be performed, provided that technical aspects such as sample mounting, sample environment, and diffraction data collection geometry are compatible with the ESB-MX capabilities.

3.1   Efficiency and user friendliness

Efficiency and user friendliness refer to the following aspects:

- Limited loss of FEL-beamtime due to change of experiment conditions, such as sample environment conditions, photon energy, photon beam size at the sample, detector geometry.

- Clear definition of supported pins for sample delivery, which will allow straightforward planning and execution of measurement campaigns. Supported pins include standard pins, as well as special pins that may be made available to the users.

- Compatibility with sample preparation and measurement procedures applied at the PX beamlines of the SLS, which will allow joint SLS and SwissFEL measurement campaigns.

- Dedicated DAQ interface, which is crucial to perform the complicated sample scans that are specified as project objectives.

- High-throughput thanks to automation of the sample exchange and to the 100 Hz sample positioning and frame acquisition.

3.2   Sample environment

The sample environment for the ESB-MX instrument is specified in the project objectives. The sample can be maintained in <u>air</u>, in which case the experimental chamber can be opened to a certain extent, or in <u>helium</u> atmosphere, in which case the chamber is closed, and the diffracted photon reach the detector through a Kapton exit window. The time required to change from the air to the helium atmosphere setup is expected to be of the order of 1 hour.

In both environments, the protein samples can be measured at <u>room temperature</u>, or at <u>cryo-conditions</u>, ensured by blowing a cryo-jet of either cold nitrogen gas or cold helium gas onto the sample, depending on whether the measurement is performed in air or helium.

3.3   Sample motions for data collection

For data acquisition, the sample will be mounted on a pin that is moved by a dedicated sample diffractometer, consisting of an omega-rotation stage with vertical axis (RΘY), supporting two translation stages (TX and TY). These translation stages are designed for fast and precise motion. The ESB-MX project objectives explicitly specify two kinds of sample motions:

- <u>100 Hz serial scanning data collection:</u> The most complicated motion required is illustrated in Figure 3. The XFEL pulses hit the sample every 10 ms. The sample chip will

be translated transversely along a "slalom trajectory" such that each XFEL pulse hits the sample within 1.2 μm from the targeted position. Translations of up to 100 μm between two pulses are achievable, and the precision of the motion is guaranteed over an area of at least 10 x 10 mm^2. During the execution of the scanning motion, the rotation stage is locked such that the sample chip surface is tilted by a fixed angle of 10º at most with respect to the beam direction. This mode of data acquisition is meaningful for samples consisting of a large number of crystals whose position has been determined previously with respect to a reference coordinate system on the sample support ("prelocation", see section 3.9). The more conventional data collection scheme based on a regular two-dimensional array can obviously also be implemented, as it is just a simpler case of the aforementioned "slalom motion". This regular scheme allows data acquisition for samples with "prepositioned" crystals (section 3.9) at the suitable grid points at potentially 100 Hz hit rate, or with randomly positioned crystals but at lower hit rate. For measurements in cryo-conditions, the sample is placed within an area smaller than 2 x 2 mm^2. Assuming a regular data collection scheme based on a regular grid with 50 μm spacing, the entire chip can be measured potentially within 16 s (chip mounting and chip orientation assessment time not included).

- <u>Synchrotron-like data collection:</u> The most involved motion takes place in helical scans, illustrated in Figure 4, which require simultaneous and synchronized translations and rotation. The images can be taken at a rate of at least at 20 Hz, translating the sample by at least 50 μm and rotating it by at least 0.5º between two successive acquisitions. The precisions in positioning the sample with respect to the beam will be better than 5 μm and 0.005º for translations and rotations, respectively. This mode of data acquisition is meaningful for crystals of size well above 50 μm, which can be hit more than once, each time at an undamaged location.
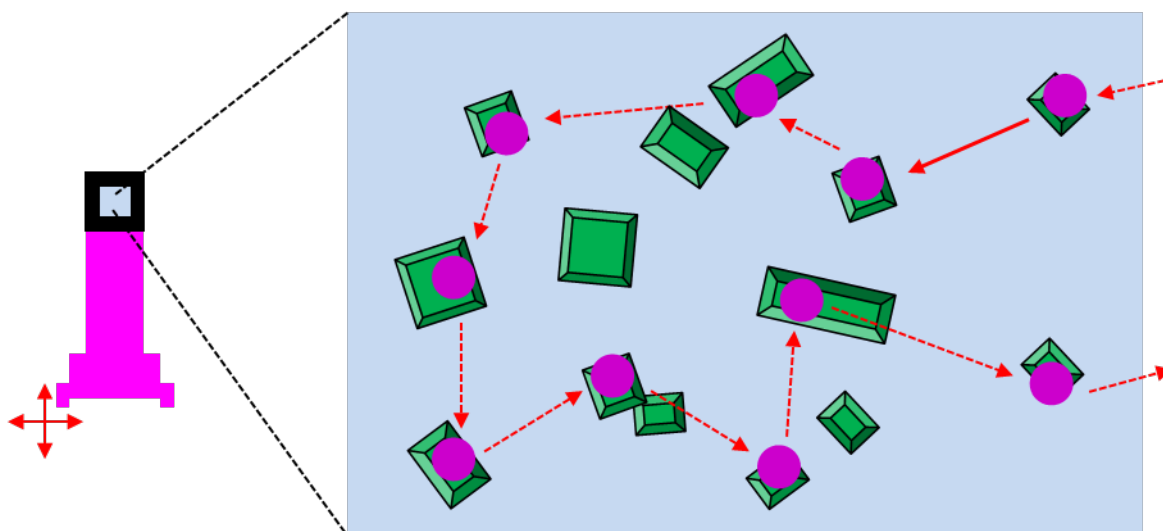
Figure 3. Serial scanning data collection.

Illustration of scanning data collection of a non-regular multi-crystal sample on a chip mounted on the pin. The shown sequence of defined X-ray hit points (magenta circles) will result in the most complicated stage translation trajectory to be implemented ("slalom trajectory"). Simpler trajectories, such as the sampling of a regular array on the sample support, are obviously possible. Specifications on translation motions are given in the text.
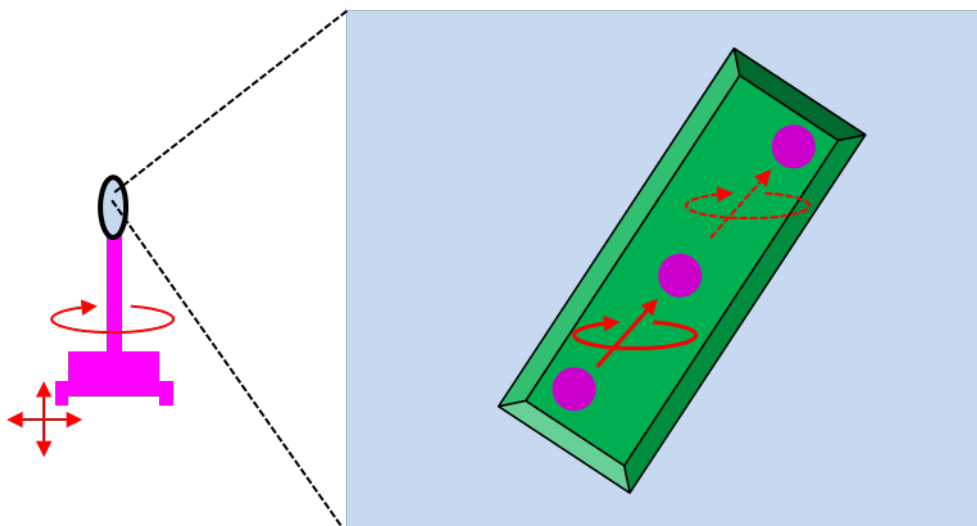
Figure 4. Synchrotron-like data collection.

Illustration of helical scans on a large crystal mounted on a loop. The rotation axis of the sample stage is vertical, while the translation direction is arbitrary. The magenta circles represent subsequent X-ray hit points. The specifications of the translation and rotation motions are given in the text.

3.4 Sample delivery pins

Several types of sample delivery pins will be employed at the ESB-MX fixed target instrument, all mountable on a same magnetic-based sample pin holder. Figure 5 gives an overview of the most relevant options that are supported.

To achieve the precision in sample positioning with the motions described in Section 3.4, a new design for the pin base will be developed that ensures sufficient stability against transverse acceleration when mounted on the sample pin holder, thus guaranteeing the specified chip positioning precision for the motion ranges shown in the figure. Two versions are foreseen in the baseline, both for a standard chip thickness of 0.2 mm. The first is designed for cryogenic measurements, with rigid chips of 5×5 mm^2 frame dimensions and an active area of 2×2 mm^2 that is small enough to be kept at cryogenic conditions within the cryo-jet stream. Silicon nitride windows in a silicon frame are a typical example. This pin variant will be compatible with the Unipuck storage and transport system. The same pin base can also be used for larger chips measured at room temperature. The second is designed for room temperature measurements only. It can accomodate chips of size up to 12.5×12.5 mm^2 with positioning precision guaranteed within a 10×10 mm^2 area, as well as larger chips of size up to 12.5×25.0 mm^2, if the positioning precision requirements can be relaxed.

To ensure compatibility with protocols followed at the Swiss Light Source and other synchrotron facilities, the ESB-MX magnetic sample pin holder will be designed to be compatible with mounting of the standard Spine pins and the MiniSpine pins under development at EMBL [37], transported in Unipuck and MiniSpine pucks, respectively. Crystals can be mounted in loops or on chips. With these pins, the precision of the sample positioning is neither specified nor guaranteed.

Finally, custom user sample supports will be accepted, provided that these are compatible with the ESB-MX boundary conditions given by the magnetic head, the mounting procedure and the space available around the sample position.
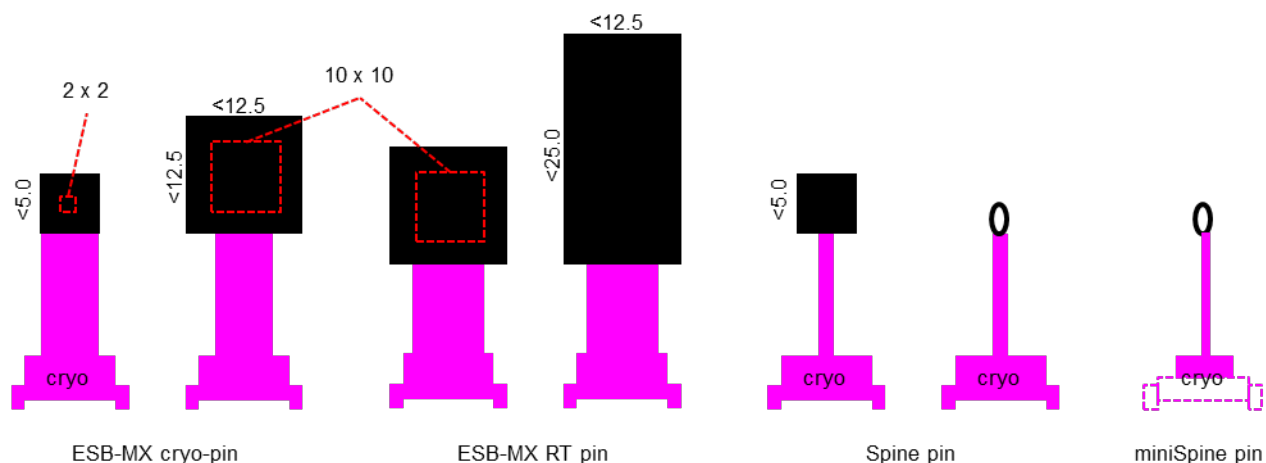
Figure 5. Supported sample pin types.

Illustration of the most relevant sample pin types supported at ESB-MX. The pin bases are in magenta, and the black rectangles represent the solid supports to mount the crystals. The small black ovals represent more traditional PX loops. Pins compatible with cryogenic mounting (gripper with walls) and data collection (cryo-jet compatibility) are indicated. The red-dashed squares represent the areas on which the specifications on the sample positioning precision are guaranteed. All dimensions are given in mm.

3.5   Sample storage and sample mounting/exchange

Figure 6 sketches the main parts of the standalone ESB-MX sample changer unit. The robot with the gripper mounted at the free end will dismount a measured sample pin and remount a new one within less than 206 s in total. For operation in helium atmosphere, the gripper will enter the chamber through a dedicated gate valve. The liquid nitrogen dewar will store 500 pins in Unipucks or 1000 pins in MiniSpine pucks in liquid nitrogen. Dry mounting is foreseen for cryogenic pins. The room temperature hotel offers space for at least 30 pins placed on Unipuck base presentation scheme. The resulting sample capacity is expected to cover at least 6 hours of operation. The whole sample changer unit will be designed for high-reliability. Furthermore, recovery procedures will be implemented, both with the goal of minimizing staff intervention and waste of beamtime. More technical details on the foreseen sample changer design are given in Section 5.4.
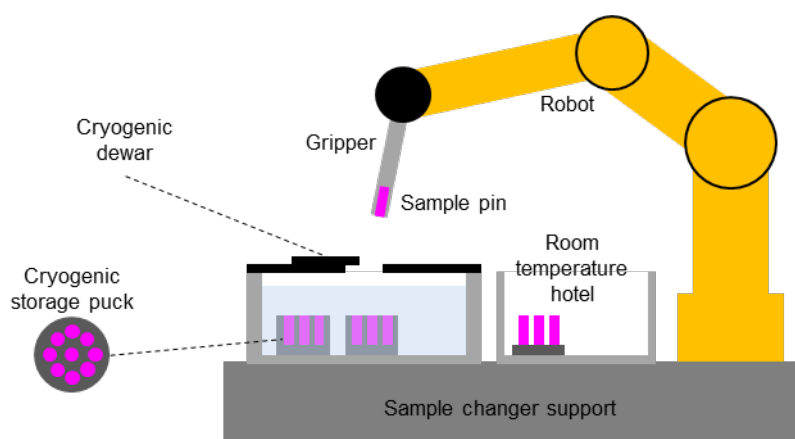
Figure 6. Concept of the sample changer unit.

3.6 Diffraction data collection geometries

The experimental chamber will be designed such that for in-air measurements the diffracted X-ray signal included within a "pyramid" of 120⁰ aperture is accessible downstream the chamber. Figure 7(a) displays the standard detector configuration. When the detector is positioned at the closest distance of 100 mm downstream the sample, better than 1 Å resolution can be achieved with an X-ray photon energy of 12.4 keV. Figure 7(b) shows an alternative detector positioning scheme, which allows finer sampling of the reciprocal space at the price of reducing the accessible reciprocal space range. Figure 7(c) shows the standard configuration for in-helium measurements. The detector can be placed 125 mm downstream the sample, after an exit window that closes the chamber. In this configuration, the achievable resolution is better than 2.5 Å with X-ray photon energy of 5.0 keV. Displacing the detector further downstream is possible, but implies that the diffracted photons travel longer distances in air, which is inconvenient due to the higher absorption in air at the lower energies.
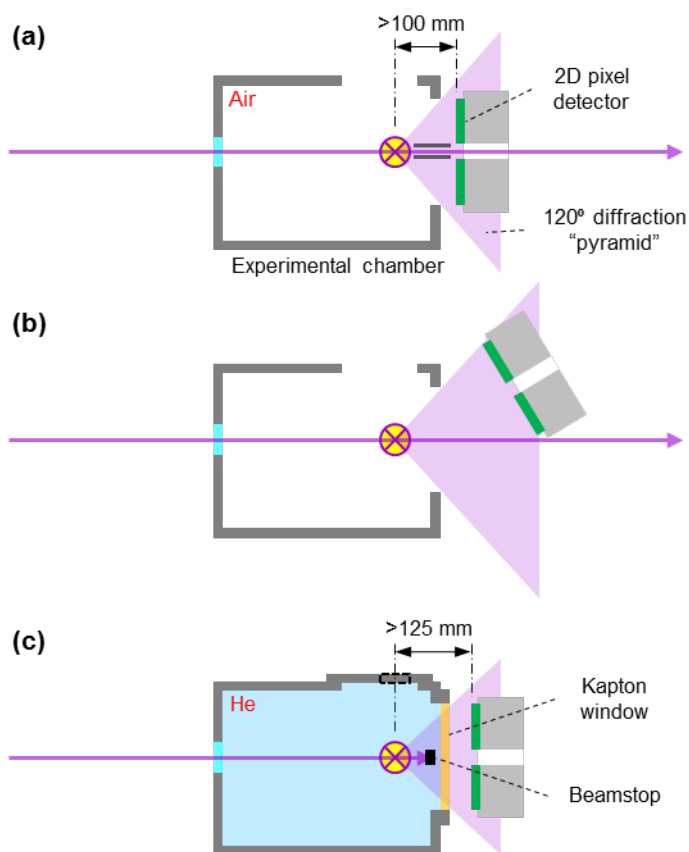
Figure 7. Diffraction data collection geometries.

Sketch in side view of the most relevant geometries to acquire the diffraction signal from the sample, represented as a violet-yellow marker. (a) Standard in-air geometry, where the direct beam passes through a post-sample tube and through a hole in the detector. (b) In-air geometry where the detector is displaced laterally and downstream. (c) Standard in-helium geometry, where the direct beam hitting a beamstop inside the experimental chamber.

3.7   Sample visualization

The design of the ESB-MX instrument foresees an on-axis microscope to visualize the sample from upstream in the same direction as the incoming X-ray beam. The resolution at the highest magnification and the field of view at lowest magnification are specified to be better than 1.2 μm and at least 1.5 mm, respectively. More details on the design concept are given in Section 5.1. The microscope camera will be capable of 100 Hz frame readout rate, thereby allowing to record diagnostics images of each exposed sample. The sample will be illuminated from upstream and downstream.

3.8   Crystal prepositioning and prelocation

Knowledge of the crystal position on a solid support prior to data acquisition in the fast scanning mode is crucial to enhance the hit rate. It can be achieved by two different approaches, both of which assume that the sample is preserved between the time of crystal position determination and the data collection.

In the "prepositioning" concept, the crystal positions are defined "offline" during the preparation of the sample. Typically aim will be to achieve crystal locations close to a regular array to simplify the scanning trajectories.

In the "prelocation" concept, the crystal positions are determined after the sample has been prepared, which typically results in a random position pattern that requires more complicated trajectories such as that shown in Figure 4. Prelocation can take place "offline", without time pressure any time before the sample is mounted for data collection, or "online", when the sample pin is mounted on the sample diffractometer and is ready to be measured. In the latter case, the time dedicated to the online prelocation is at the expense of the actual measurement time, and is therefore to be kept at a minimum.

Prepositioning and offline prelocation could take place at the home laboratory before the samples are shipped in cryogenic Dewars to the SwissFEL facility, or right before the sample is taken into the experimental chamber. Both require fiducial marks on the chip, which serve as reference points to align the chip in the beam (Section 5.2.3.3). The markers are not strictly necessary for the online prelocation approach, but may nevertheless be of help for easier chip alignment.

The development of suitable preposition and prelocation methods is not an objective of the ESB-MX project. However, it is planned to investigate the following options:

- Prepositioning of crystals on holes in a silicon chip [14]
- Offline prelocation by SONICC [1]
- Offline prelocation by UV fluorescence [17]
- Offline prelocation by X-ray phase contrast imaging
- Offline / online prelocation by polarized visible light microscopy

3.9   X-ray beam parameters

The photon energies for operation of the ESB-MX instrument are specified in the project objectives to include at least the range 5.0 – 12.7 keV. The values of other beam parameters that are taken into account for the instrument design correspond to the parameters at the ESB station.

At the ESB sample position, it is predicted that the X-ray beam can be focused down to 3 and 2 μm FWHM at 5.0 and 12.4 keV respectively. Defocusing is done by adjusting the beamline KB focusing mirrors. The apertures on the X-ray beam path of ESB-MX instrument will be designed to accommodate a beam size of 20 μm FWHM at the sample position for the defined photon energy range. In the standard SASE mode, the X-ray pulse length can be tuned in the range 2 – 21 fs RMS (5 – 50 fs FWHM).

The ARAMIS-2 beamline can be operated in pink-beam mode ($2\cdot10^{-3}$ relative bandwidth), using two horizontal harmonic rejection offset mirrors, or in monochromatic mode, after removing the mirrors from the beam path and employing a vertical two-bounce Si(111) monochromator. The highest pulse energy is achieved in pink beam mode, which will be used for most PX applications, for the longest 21 fs pulses. At 5.0 keV and 12.0 keV, taking into account the transmission of the various optical elements and assuming helium sample environment, one expects about 0.5 and 0.4 mJ per pulse ($6.5\cdot10^{11}$ and $4.0\cdot10^{11}$ photons/pulse), respectively at the sample position. The corresponding values at 6.0 and 12.4 keV in air environment are about 0.2 and 0.7 mJ per pulse ($2.0\cdot10^{11}$ and $3.5\cdot10^{11}$ photons/pulse), respectively, again with the longest 21 fs pulses. For more details on pulse parameters see Appendix 7.2.

3.10   Data evaluation and crystallographic data analysis

The SwissFEL facility will provide IT resources to monitor in almost real-time the data acquisition on all active detectors, including those incorporated in the ESB-MX instrument, and to perform intensive offline PX data analysis within times useful to define subsequent steps during the measurements. The currently used programs in the PX XFEL community will be available.

4 ESB-MX instrument layout

This section describes the overall layout of the ESB-MX instrument, as well as the integration of the instrument at a hosting experimental station. In its early days in particular, the ESB-MX instrument will be installed at the SwissFEL ESB station for dedicated 5 – 6 day measurement campaigns.

4.1 ESB-MX main components

The following main physical components of the ESB-MX instrument, including their most relevant connections, are sketched in Figure 8:

- Experimental chamber: includes the sample diffractometer, as well as the elements to monitor the sample (cameras, illumination), to condition the X-ray beam (slits, collimators), to monitor the X-ray beam position (scintillation screens), and to control the helium pressure inside the chamber for in-helium operation;

- Cryo-jet: includes the cryo-jet nozzle, which intrudes into the chamber and blows cold N_2 or He gas onto the sample, the compressor and the refrigerator.

- Sample changer: includes a robot with a sample gripper to mount samples through a valve in the experimental chamber, a liquid nitrogen Dewar to store the samples at cryogenic conditions, an enclosure to store the samples at room temperature, and a small rack for control of the robot motion and of the liquid nitrogen level in the Dewar.

- Electronics rack: will include all the electronics required to operate the ESB-MX instrument except the servers for the cameras and the sample changer controllers.
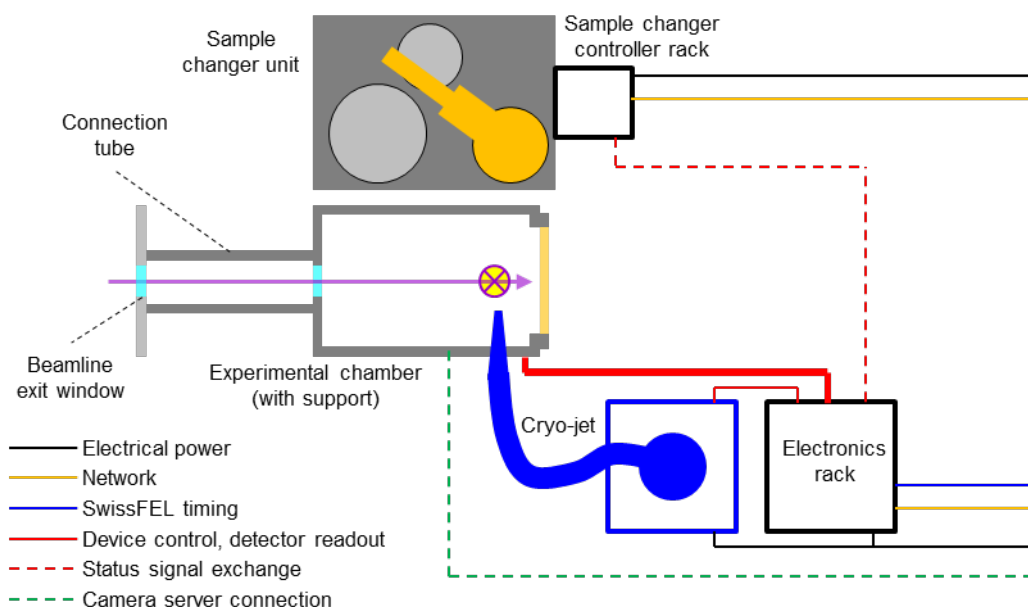
Figure 8. ESB-MX main components.
The sketch in top view shows the main components that are part of the ESB-MX instrument. Various types of connections are indicated in different colors / linestyles.

4.2   External devices required for ESB-MX operation

The ESB-MX instrument is not a standalone unit, but requires a number of external devices and infrastructure that must be available at the station hosting the instrument. The additional devices and infrastructure are:

- X-ray pixel array detector to record diffraction images: 16M Jungfrau detector mounted on a robot arm.

- Optics components: offset mirrors (safety elements and harmonic rejection), pulse picker to define the sub-100 Hz pattern of the pulses reaching the sample, attenuators, KB focusing mirrors.

- Non-invasive X-ray photon diagnostic devices, all working on single-shot basis at 100 Hz: gas-based absolute intensity monitor, spectrometer, beam position and relative intensity monitors upstream and downstream of the sample.

- Pump-laser (for pump-probe experiments): laser optics table, timing-tool(s)

- Media: liquid nitrogen pipe and cold nitrogen gas exhaust for sample changer, nitrogen and helium gas for the cryo-jet, water-cooling system for the cryo-jet compressor, compressed air for sample changer robot, cold helium gas exhaust or recovery line.

The needs are covered by the infrastructure available on the ARAMIS-2 beamline and at the ESB station. Figure 9 sketches the relevant X-ray beam related devices.
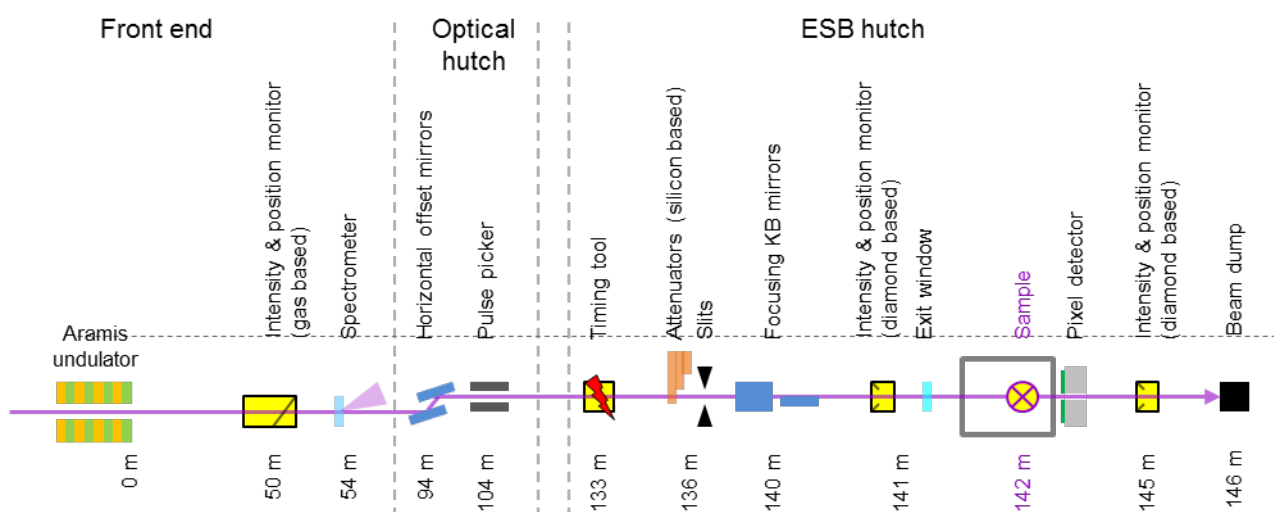
Figure 9. External X-ray beam related devices.

The sketch shows the most important devices required to operate the ESB-MX instrument, which are included in the ARAMIS-2 and ESB infrastructure. The approximate distances from the source point at the end of the ARAMIS undulator are indicated. The timing tool is required only for pump-probe experiments foreseen after upgrade of ESB-MX. The horizontal mirrors can be replaced with a double crystal Si(111) monochromator for narrowband operation.

4.3   Integration of ESB-MX at ESB

Figure 10 shows the physical integration of the ESB-MX equipment within the ESB infrastructure. The experimental chamber will be fixed on a heavy support anchored on slides mounted on the rails that are fixed to the floor. This allows rough horizontal positioning in the direction transverse to the beam. The sample changer unit will be anchored to the floor on the left hand side of the experimental chamber. The other equipment will be placed on the free floor space available around the sample position. The 16M Jungfrau detector can be positioned in a wide range of positions downstream of the chamber due to a long robot detector arm, and in particular sufficiently close to the chamber to reach the resolution specifications.
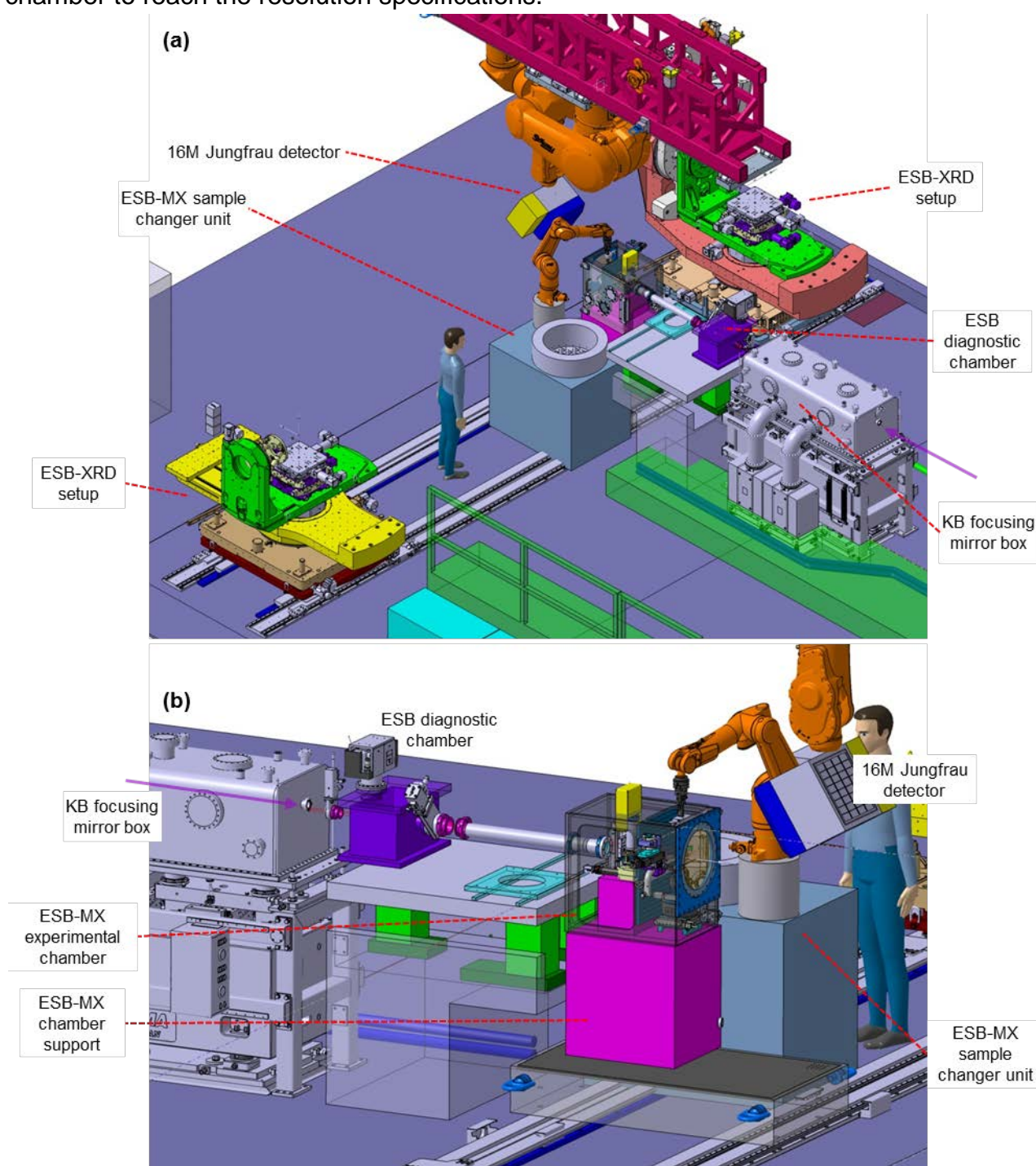
Figure 10. ESB-MX layout at ESB.

Layout of the ESB station with the ESB-MX hardware in its foreseen position. The relevant components are labeled. (a) Overall view: The ESB-XRD and ESB-GPS instruments are parked on the side at the end of the rails. (b) Magnified view of the ESB-MX instrument. The 16M Jungfrau detector can be moved and positioned right downstream of the experimental chamber.

5   Technical aspects

This section describes the concepts to address the most relevant technical challenges faced within the ESB-MX project, which are presented according to the project workpackage organization illustrated in Figure 11 (see also Table 12).
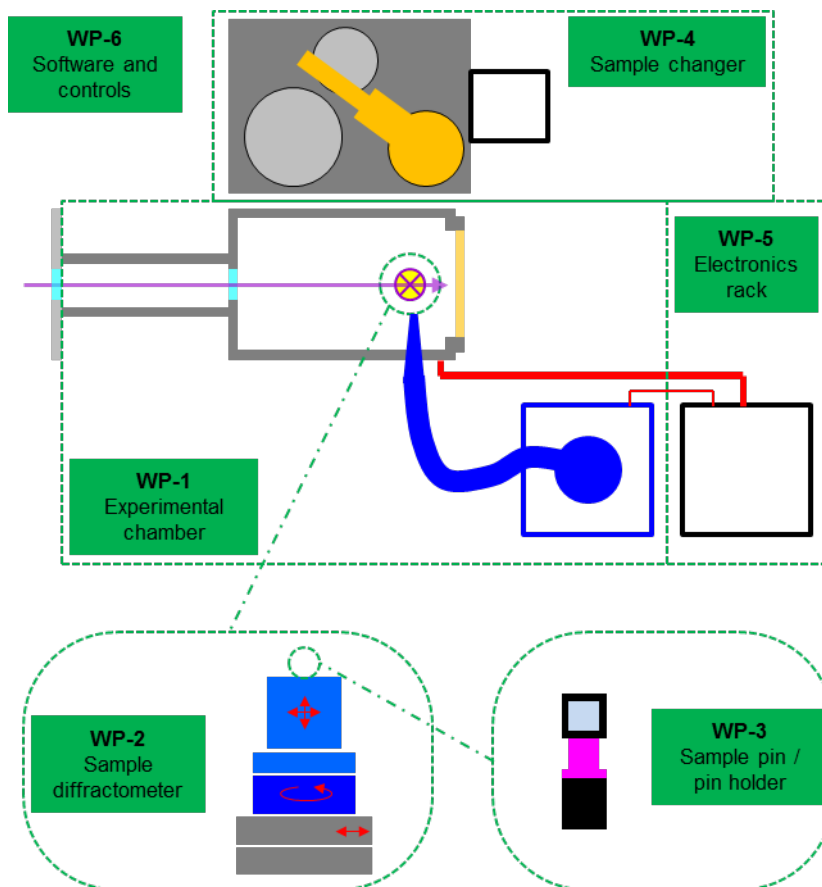
Figure 11. ESB-MX workpackages.
Characterization of the ESB-MX workpackages with sketches of the ESB-MX hardware.

5.1   Sample diffractometer (WP2)

Section 3.4 describes the type of motions the sample stages have to perform, as well as the precision for the motions to be implemented. The total mass of the sample pin and the sample pin holder that has to be moved, not including the sample stages, has been specified to 100 g at most.

For the "scanning data collection", an overall position error budget is reported in Table 2. Achieving an overall positioning error of 1.2 μm leaves only 200 nm error for the XY motion. The complicated time-evolution, which has to be synchronized with the SwissFEL X-ray pulses hitting the sample at up to 100 Hz, makes it a challenge to meet the specifications. Therefore, already at the present stage of the project, an almost final design of the sample diffractometer has been made. The design concept is sketched in Figure 12, which makes both data acquisition motion types possible. The sample stage part consists of two translation stages (TX2 and TY2) mounted on top of a vertical rotation stage (RΘY). Relying on a vertical axis design

instead of a horizontal axis design for the rotation stage enhances the overall stability. The TX2 and TY2 stages perform the sample transverse displacements. They will be equipped with an interferometer providing absolute position feedback to correct for positioning errors in real-time and achieve the desired positioning precision. The interferometer is mandatory, as the most precise commercial stages will not meet the requirements. Two closed control loops for position and velocity will be implemented. The whole sample stage will be mounted on a stiff TX1/TZ1 stage for overall positioning and alignment purposes. A spacer is inserted between the TX2/TY2 and RQY stages, and will be replaced by a third translation stage TZ2 only in the case that the wobbling corrections of the rotations cannot be achieved with the TX1/TZ1 and the TX2 stages to the specified precision. Figure 13 shows the design of the sample diffractometer. Suitable commercial products have already been identified. The motion ranges and resolutions are given in Table 3.

	Error source	Error type	Error estimate
Mechanical	Translation stage motion	Random	200 nm
	Chip position determination	Systematic	500 nm
	Recoil from stage motion	Random	200 nm
	Ambient vibrations (floor, air, …)	Random	100 nm
Other	Transverse beam position jitter	Random	300 nm
	Crystal prelocation, random	Random	200 nm
	Crystal prelocation, systematic	Systematic	200 nm
Total			1170 nm

Table 2. Positioning error budget.

Estimate of the errors from different sources for the positioning of the sample in the X-ray beam in the fast scanning data acquisition mode. Systematic errors are added to the total error from random sources, calculated as the square root of the sum of squares.
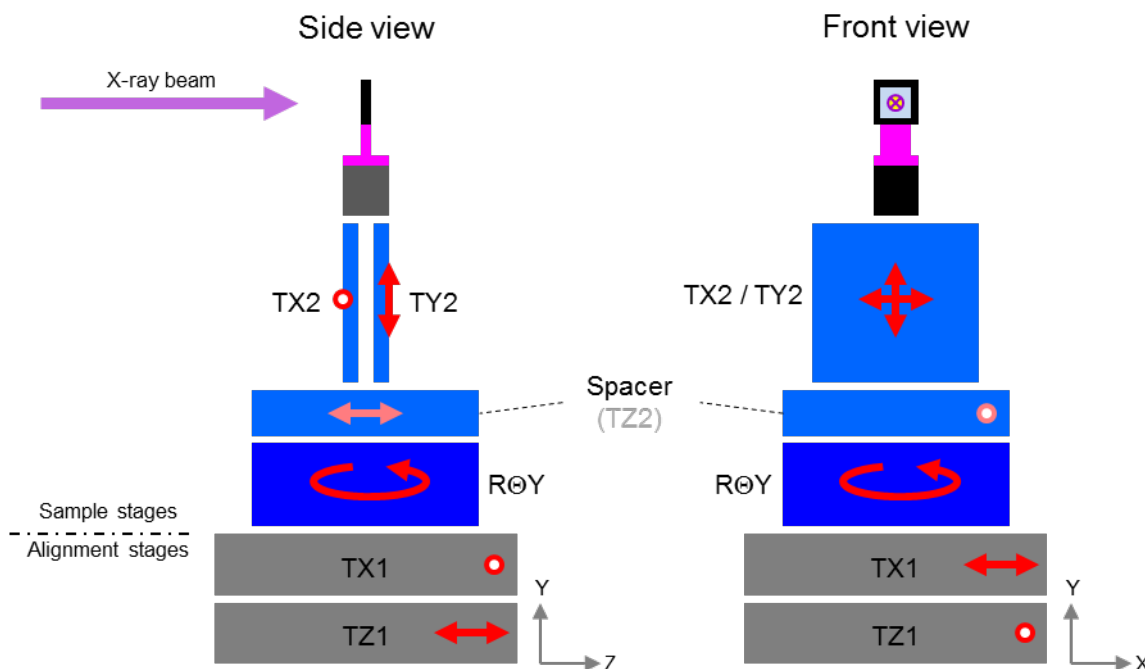
Figure 12. Diffractometer layout concept.

The sketch shows the diffractometer stages in side and front views. The sample pin is mounted on top. Stages motions are indicated by red arrows. The sample stage includes the fast TX1 and TY1 translation stages with interferometric feed-back motion and the vertical

axis RΘY rotation stage. The spacer will be replaced by the TZ2 translation stage only if necessary. The alignment stage includes the TX1 and the TZ1 translation stages.
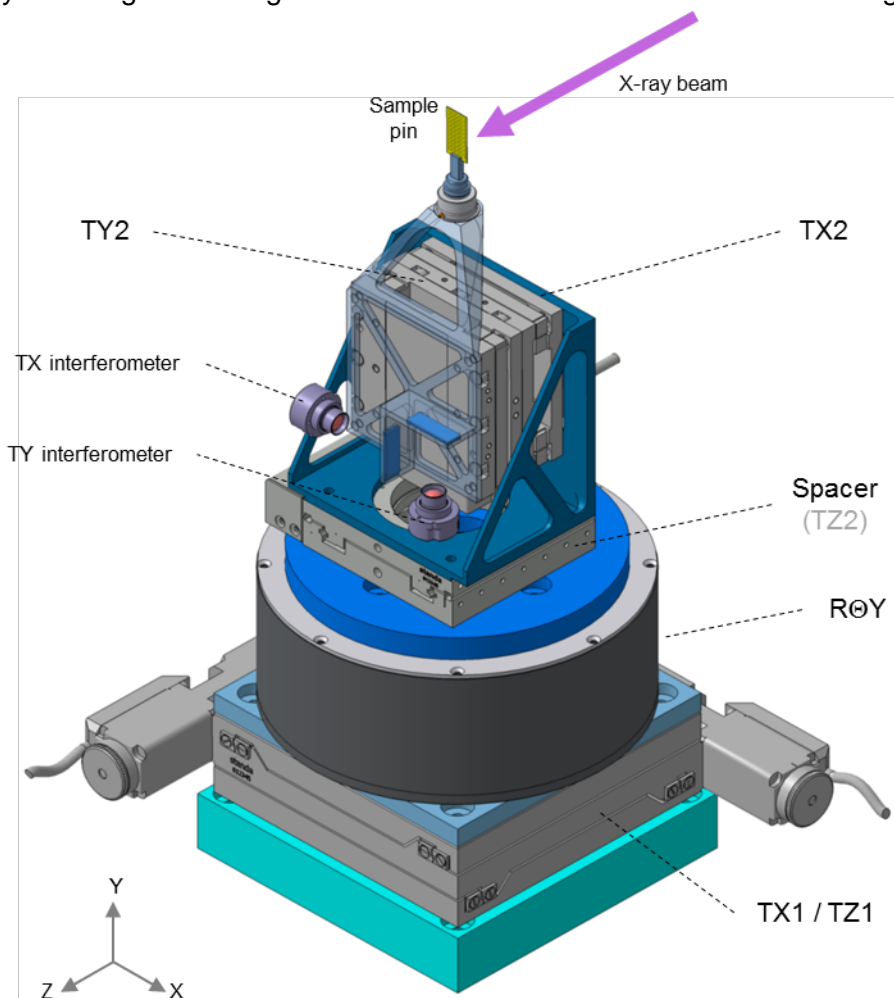
Figure 13. Diffractometer design.
The design corresponds to the layout of Figure 12.

Stage	Type	Use	Range	Resolution	Provider
TX2	Servo	Sample translation, scans and	± 12.5 mm	0.02 μm	Parker
TY2	Servo	helical scans	± 12.5 mm	0.02 μm	Parker
RΘY	Servo	Sample rotation, helical scans	> ± 180º	0.00034º	Parker
TX1	Step	Sample stage alignment, wobble	± 37.5 mm	2.50 μm	Standa
TZ1	Step	correction for rotations	± 37.5 mm	2.50 μm	
TZ2	Step	Sample alignment, helical scans	± 12.5 mm	1.25 μm	Standa

Table 3. Diffractometer stages characteristics.
The stages are labeled according to Figure 13 and Figure 14. The TZ2 stage will be included only if necessary.

5.2 Sample pin and sample pin holder (WP3)

5.2.1 Overview

The different parts related to the workpackage WP3 have been named as shown in Figure 14. The sample pin consist of a chip (or equivalent support) on which the sample is deposited, fixed onto a stiff mechanical support. The sample changer mounts the sample pins onto the sample pin holder, which is attached to the TX2/TY2 sample translation stage.

The sample pin is kept in position by magnetic forces acting on the pin base. A holder acting by magnetic instead of mechanical forces is chosen because of precision issues and because of compatibility with standard solutions widely spread in the protein crystallography community (Spine and miniSpine).

Figure 14. Sample pin and sample pin holder.
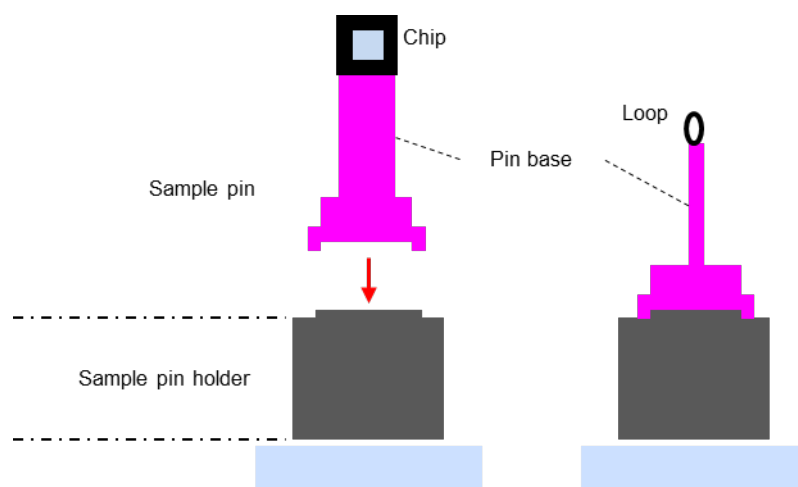Naming of the parts for the special ESB-MX pin with chip (left) and for a standard Spin pin with a loop (right).

5.2.2 Sample pin holder

For the sample pin holder, the choice is between permanent- and electromagnet-based systems. Table 4 lists the pros and cons for the two options. The electromagnet-based solution has important practical advantages, in particular it offers sample detection even for operation in the dark. The sample stages can accomodate the cables to control the electromagnet force. A novel commercial solution for an electromagnet-based device compatible with Spine and miniSpine pins has been identified. This solution will be pursued if confirmed to be compatible with the specifications of the ESB-MX project. In particular the holding forces must be strong enough to avoid sliding of the pin on the pin holder during "slalom motion". It is emphasized that any sample pin holder can be replaced with minimal effort, in case a more convenient solution becomes available in the future.

Magnet type	Permanent magnet	Electromagnet
Complexity	Low (no control cables)	High (cables through sample motion stages)
Holding force	Strong	Generally weaker
Sample exchange	Strong force to remove pin	Easy sample exchange by controlling the magnet current. Higher flexibility in mounting procedures.
Sample detection	Challenging	Possible (even in the dark)

Table 4. Permanent magnet- and electromagnet-based pin holders.

The table summarizes the pro and cons of the two solutions for magnetic based holding of the sample pin.

5.2.3   Special ESB-MX sample pins

In Section 3.5 various sample pins that can be employed for measurements at the ESB-MX station have been listed. In the following, more details are given for the special sample pins that will be developed within the ESB-MX project. The present design concept is shown in Figure 15.
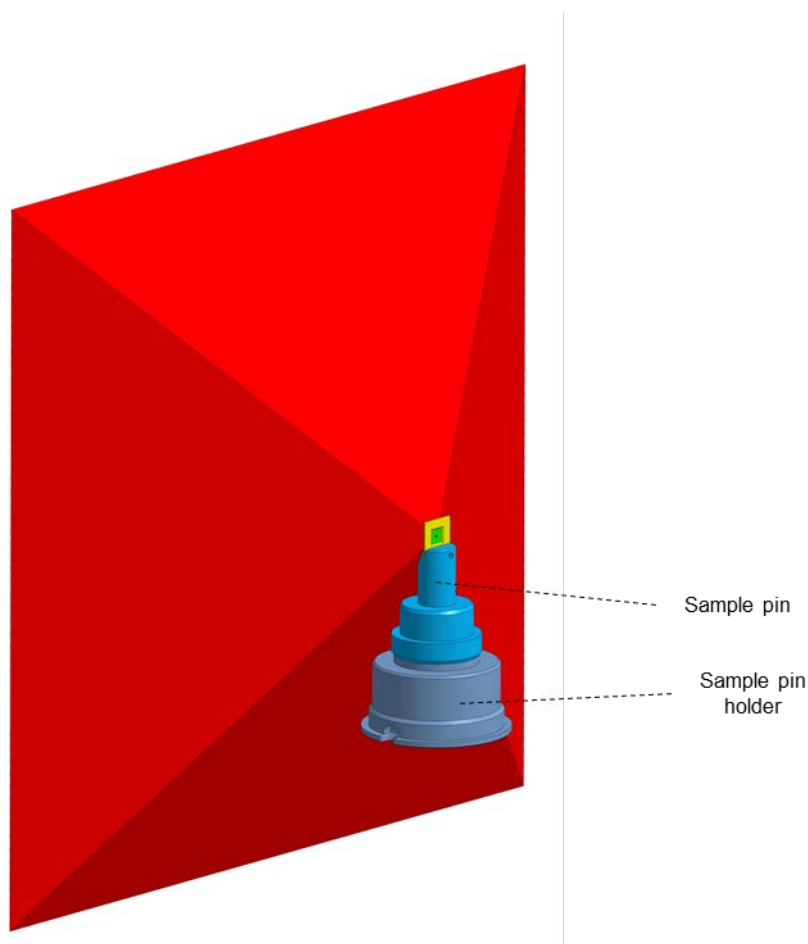
Figure 15. Special ESB-MX sample pin design.

The technical drawing shows the pin for cryogenic measurements, mounted on top of the sample pin holder. The red volume represents the 120⁰ aperture diffraction pyramid that is specified to reach the detector.

5.2.3.1   Sample pin for cryogenic measurements

The cryogenic temperature pin is designed for mounting chips with dimensions 5 x 5 x 0.2 mm^3, and active area 2 x 2 mm^2 with the center at the defined standard beam position, 18 mm above the sample pin holder top surface (Figure 16(a)). The specified frame dimensions of 5.1 +/- 0.2 mm were derived from measurements on commercial chips from Silson (reference 11505107 PRS 3914).

The dimensions of the base are defined to meet the following requirements:

- Compatibility with mounting on the pin holder

- Compatibility with gripping by the robot (cryogenic temperature gripper) at the shoulders or from below
- Compatibility with storage and transport of the sample-pin assembly in Unipuck

This naturally leads to take over the relevant dimensions of the standard Spine magnetic base. The chip is fixed to the base via a cylinder-shaped body of 5 mm diameter, which must be rigid enough to allow fast scanning. The overall dimensions at sample position must be such that the flow of the cryo-jet is not perturbed significantly. The cryogenic pin can also be used to mount larger chips for room temperature measurements (Figure 16(b)).

5.2.3.2   Special room temperature pin

The room temperature pin is used for mounting chips with different dimensions. For the 12.5 x 12.5 x 0.2 mm^3 chip shown in Figure 16(c) precise positioning during 100 Hz scanning data collection will be ensured with the X-ray beam inside a 10 x 10 mm^2 area. The height of the pin is such that the center of the 12.5 x 12.5 x 0.2 mm^3 chip corresponds to the standard distance of 18 mm from the sample pin holder top surface (Figure 16(c)). The pin can also support chips of size up to 12.5 x 25 x 0.2 mm^3 (Figure 16(d)), however without guarantee on positioning precision during 100 Hz scans.

The dimensions of the base are defined to meet the following requirements:

- Compatibility with mounting on the pin holder
- Compatibility with gripping by the robot (room temperature gripper) at the shoulders or from below
- Compatibility with the pin positioning scheme on a Unipuck base, and accessibility by the gripper.

This naturally leads to take over the relevant dimensions of the standard Spine magnetic base. The chip is fixed to the base via a solid body that must be rigid enough to allow fast scanning of the 12.5 x 12.5 x 0.2 mm^3 chip.
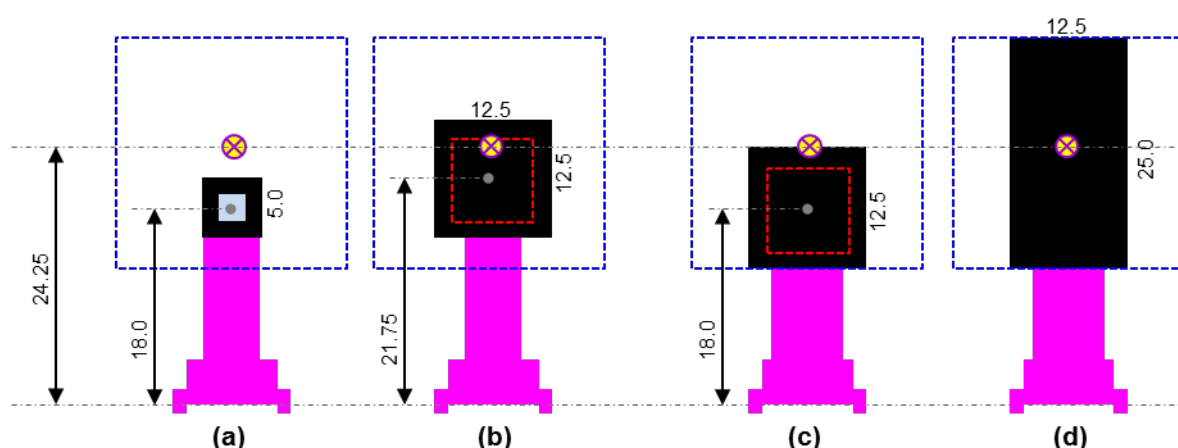
Figure 16. Special ESB-MX sample pins.

Schematics of the position of the chips on the cyogenic pin (a,b) and room temperature pin (c,d), with respect to the available scanning area of the TX2 and TY2 stages (Figure 12) represented by the dashed blue square. The yellow-violet mark represents the beam position when the translation stages are in neutral position. The dimensions are given in mm. (a)

represents the configuration for measurements with cryo-cooled samples, with the 2 x 2 mm^2 sample area in grey. (b-d) are possible configurations for room temperature (RT) measurements, with the dashed red squares represent a 10 x 10 mm^2 area in which the positioning precision for 100 Hz data acquisition is guaranteed.

5.2.3.3   Precise positioning of chips

The precise assessment of the position of a chip with respect to the X-ray beam is essential before starting scanning data acquisition with chips on which the crystals have been "prepositioned" or "prelocated offline" (see Section 3.9). The positions of known markers on the chip has to be determined, and will serve to determine the transformation between the coordinate system of the chip and the coordinate system of the sample stages. Table 5 summarizes the options foreseen for the ESB-MX instrument, which require the implementation of special markers directly on the chip.

Marker type	Contrast mechanism	Position detection procedure
Visible dot	Visible light transmission / reflection	Establish position of dot with microscope image
Shaped visible feature	Visible light transmission / reflection	Feature recognition on microscope image to enhance resolution in position
Window edges / corners, holes in chip	X-ray absorption	X-ray scanning of marker with translation stage, monitoring of transmitted X-ray intensity
Fluorescent dot	X-ray fluorescence	X-ray scanning of marker with translation stage, monitoring of fluorescent intensity at longer wavelength
Polycrystalline dot	X-ray powder signal	X-ray scanning of marker with translation stage, monitoring of powder signal (rings on detector

Table 5. Options for chip positioning.

5.3   Experimental chamber (WP1)

5.3.1   Chamber layout overview

A sketch of the concept for the experimental chamber concept is represented in Figure 17, and a list of components is given in Table 6.
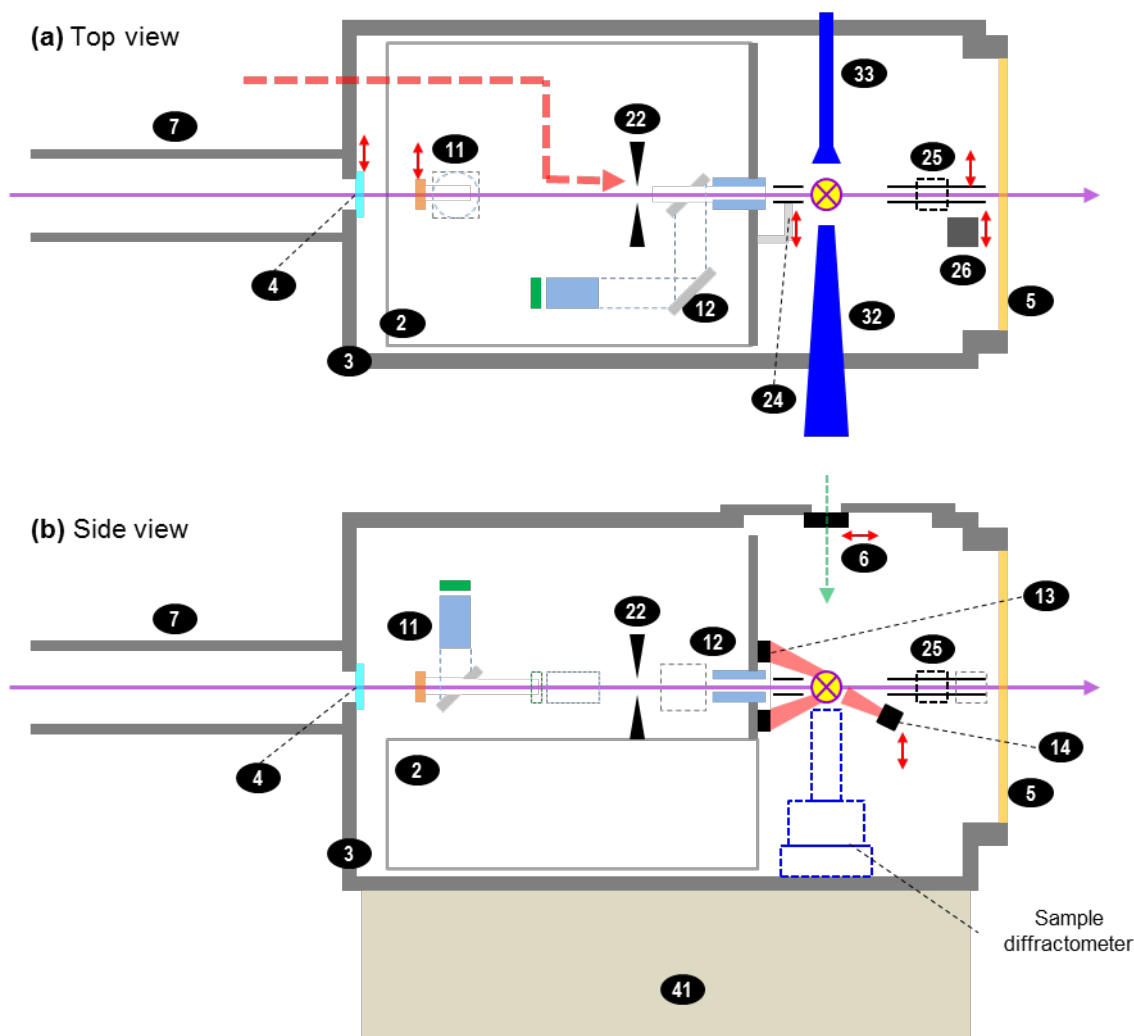
Figure 17. Experimental chamber layout.

Sketch of the foreseen layout of the experimental chamber. The numbered components are described in Table 6. The red arrows indicate retractable components. (a) Top view: the red dashed line is the incoupling path for the pump laser foreseen as an upgrade of the instrument. (b) Side view: the dashed green line represents the gripper path during sample pin mounting.

	Component	Function	Remarks
2	Supporting board	Supports and aligns all beam components upstream of the sample.	(Eventually used to align the supported components to X-ray beam)
3	Chamber	Device enclosure, helium atmosphere enclosure.	Some walls can be opened for in-air operation.
4	Chamber entrance window	Closed/Open for in-air/in helium operation	
5	Chamber exit window	Encloses helium atmosphere, almost transparent to diffracted X-ray signal	Can be dismounted for in-air operation
6	Gate valve	Opens to allow sample changer gripper access for in-helium operation	
7	Connection tube	Encloses beam path from ESB beamline diamond exit window to ESB-MX chamber	
11	X-ray profile monitor	Tracking X-ray beam path	Scintillator (and eventually drilled mirror) retractable
12	Sample on-	Sample visualization	

	axismicroscope		
13	Sample front illumination	Sample illumination	
14	Sample back illumination	Sample illumination	Retractable
22	Slits	Beam cleanup	
24	Collimator	Minimization of air scattering to detector from direct beam	Retractable
25	Post sample tube / Beamstop	Minimization of air scattering to detector from direct beam for in-air operation / Stopping of direct beam for in-helium operation	Dismountable elements, either tube or beamstop or none mounted
26	Beamstop with diode	Beamstop, direct beam transmission measurement	
32	Cryo-jet	Sample cryo-cooling by cold gas jet	N_2: >77 K; He: >20 K
33	Cryo-jet sucker	Funnels cold gas flow away	
41	Chamber support	Supports chamber, includes stages to align entire chamber to X-ray beam	

Table 6. Experimental chamber components.

5.3.2   X-ray beam path and X-ray beam components

The X-ray beam exits the last beamline diamond window at the downstream end of the ESB diagnostic chamber and travels through the connecting tube until the chamber entrance diamond window, which can be open or closed. Inside the chamber, the beam passes the X-ray eye, hitting the scintillator if inserted, propagates through the beam cleanup slits, through drilled optical components of the on-axis microscope, through the collimator if inserted, and reaches the sample position. Downstream of the sample, the direct beam travels through the post-sample tube and through the detector central hole until the ESB beam stopper. The post-sample tube can be replaced by a beamstop that can block the direct beam. An insertable beamstop with a diode, to be used only with attenuated beam, will be available for X-ray transmission measurement.

5.3.3   In-air and in-helium configurations

For in-air measurements (Figure 18(a)), the exit window and other chamber windows can be dismounted. The first X-ray beam section after the ESB beamline exit window is within a connection tube, which can be filled with helium or kept in low vacuum (10^{-4} mbar) to reduce the X-ray absorption. Scattering from the direct beam into the detector is minimized by the slits, by the collimator right upstream of the sample position and by the post-sample tube downstream of the sample position.

For in-helium measurements (Figure 18(b)), the exit window is mounted and the chamber is closed. The chamber entrance window is open, resulting in a single compartment filled with helium, maintained at slight helium overpressure in the range 1 – 20 mbar with respect to the experimental hutch air pressure. The helium minimizes the scattering from the direct beam, and reduces the absorption losses of the direct incoming beam as well as of the diffracted radiation.

(a)

1300 - 1400 mm

350 – 400 mm

~ 160 mm

Helium / Vacuum (10⁻³ mbar)

Diamond windows

(b)
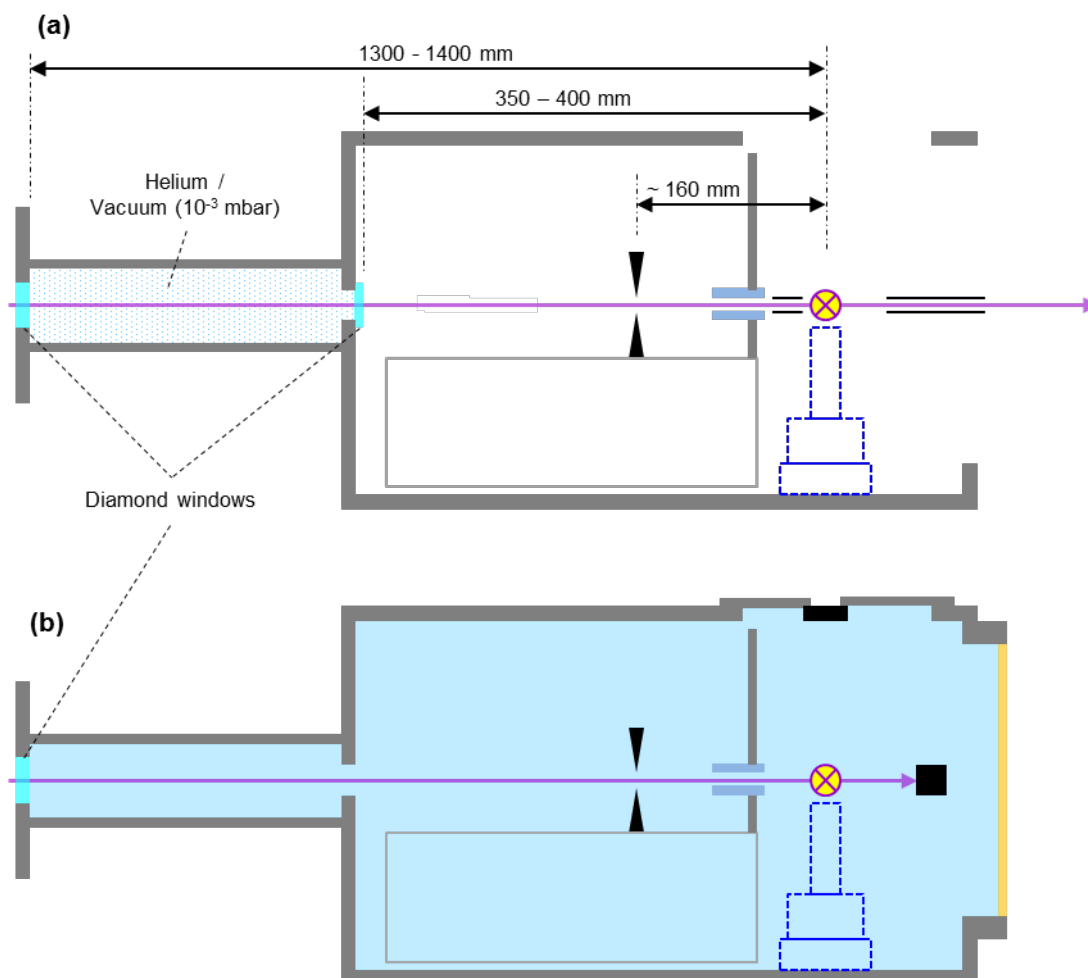
Figure 18. In-air and in-helium chamber setup.

Sketch of the experimental chamber and the relevantbeam components. (a) Setup for in-air operation. (b) Setup for in-helium operation.

5.3.4 On-axis microscope and sample illumination

The on-axis microscope specifications are given in section 3.7. The design is sketched in Figure 19, and relies on a drilled on-axis objective passed by the X-ray beam. The sample will be illuminated from upstream and downstream with a fixed and retractable RGB led lamp system, respectively.

Drilled objective

34 mm

Relay lenses

Camera

Zoom
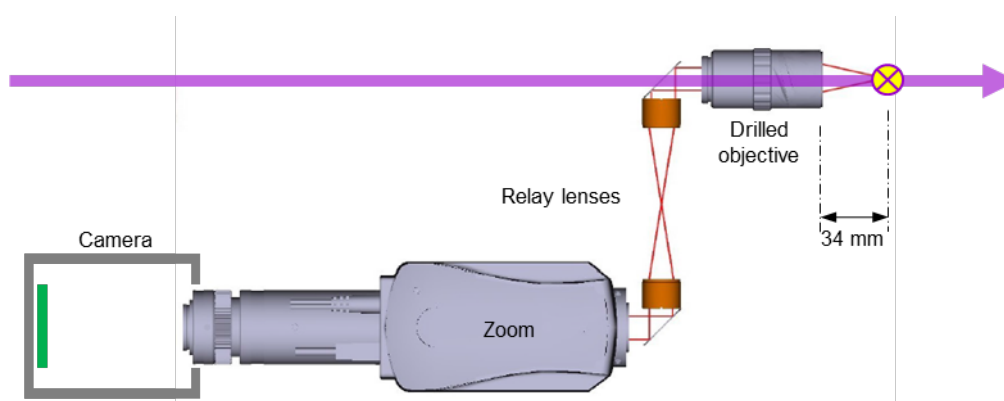
Figure 19. On-axis microscope design.

Sketch of the microscope component layout, inspired from the setup at the X10SA PX beamline at the SLS.

5.3.5   The cryo-jet

A cryo-jet setup will be chosen where all equipment is separated from the nozzle by a flexible line, which enables decoupling of mechanical vibration from the experimental chamber (Cryocool G2B model from Cryo Industries of America, Inc.). The same device will deliver a cold jet of nitrogen or helium gas, for in-air and in-helium measurements, respectively, depending on the demands of the user. The cryo-jet stream will flow horizontally, transverse to the incoming X-ray beam. Laminar flow will be maintained by a cryo-jet sucker opposite the sample position.

5.3.6   X-ray beam position tracking and chamber alignment

The transverse position of the X-ray beam through the experimental chamber can be tracked at two different longitudinal positions. The X-ray profile monitoris located 200 – 350 mm upstream the sample position in the converging beam region. Using a retractable Ce:YAG scintillator screen and with appropriate beam attenuation, the beam position will be determined with about 5 – 10 μm accuracy. At the sample position, the focused or unfocused beam position can be established to an accuracy of about 2 – 3 μm using different targets that can be mounted on pins in the same way as protein crystal sample pins. With the on-axis microscope one can visualize the fluorescence signal generated by the properly attenuated X-ray beam on a Ce:YAG screen, or the impact marks of the full beam on a metal foil. Alternatively, one can monitor the X-ray emission signal or the diffraction ring intensity from fluorescent and crystal-powder micron-sized structures, respectively, when the supporting membrane is scanned through the X-ray beam with the sample translation stages. From the two determined beam positions, the position and orientation corrections necessary to overlap the reference axis of the ESB-MX setup with the incoming beam will be calculated and implemented (see section 5.3.1).

5.3.7   Fluorescence detection

Detection of fluorescent X-ray emission intensity of specific elements with absorption edges in the photon energy range 4.0 – 12.7 keV may be required for a number of tasks, including fluorescent mark position determination, as mentioned in sections 5.2.3.3 and 5.3.6. For photon energy resolved detection, conventional electron drift based photon fluorescence detectors used at synchrotron beamlines are not suitable. Indeed, the time structure of the emitted radiation is the same as that of the incoming radiation, and therefore all fluorescent photons reach the detector in less than 100 fs and cannot be counted appropriately. Instead, it is planned to exploit the photon energy discrimination of about 1 keV built in the charge integrating Jungfrau pixel detector technology. If the incoming beam is attenuated such that the total number of photons detected in each Jungfrau pixel is well below unity, in the per-pixel charge histogram of each pulse the emission line can be discriminated from the elastic peak, allowing the quantification of the total emission intensity. For this purpose, the same Jungfrau detector that collects the diffraction signal may be used. Furthermore, the ESB-MX chamber is designed to accommodate a retractable Jungfrau sensor chip with about 50k pixels close to the sample position, if required.

5.4   Automated sample changer (WP4)

The development and realization of the sample changer unit will be realized as an independent project within the SLS-MX group. A concept will be developed for a system matching the needs

for the new ESB-MX instrument as well as for the replacement of the units at the three SLS PX beamlines. One unit includes the sample changer robot, the Dewar to store the samples in liquid nitrogen, space to store samples at room temperature, a rack hosting all control electronics, and a set of at least two different sample pin grippers (one for cryogenic mounting of the cryo-compatible pins, the other one for the larger room temperature pins).

The critical requirements common to all units are:

- High speed of exchange: less than 16 s for a full sample pin exchange cycle (well below the 20 s limit set for the ESB-MX project)
- Minimal overhead time for gripper drying and robot coordinate system calibration
- High reliability and collision recovery procedures to avoid direct human intervention during continuous measurement periods of the order of 1 week (corresponding to one ESB-MX measurement campaign at ESB)
- High capacity of the cryogenic sample storage dewar: about 500 Spine pins or 1000 miniSpine pins (corresponding to 6 hours of autonomous operation at ESB-MX).
- Low maintenance workload

The ESB-MX specific critical requirements are:

- Vertical sample pin mount
- Support of the sample changer unit and calibration/alignment procedures that allow fast installation and uninstallation at the SwissFEL ESB station.
- Positioning of the robot elements with respect to the sample position, in the absence of manual mounting
- Access of the robot gripper to the sample position through the ESB-MX gate valve for in-helium operation

5.4.1 Sample changer robot

The sample changer robot (Figure 20) will be a Stäubli TX60L model, with a reach of 920 mm and a maximal load capacity of 5 kg. The positioning reproducibility at the wrist is 30 µm, and the maximum speed at the load gravity center is 10.6 m/s. This type of robot is widely used in automatic sample changer systems for PX applications, and has been used for almost 10 years at the SLS PX beamlines. The use of an industrial robot provides more flexibility for the chip mounting trajectories compared to a linear axis-based system.

5.4.2 Sample changer Dewar

The sample changer Dewar (Figure 20) is in the concept phase. Already defined features are the use of a steel, vacuum-insulated tank, and an indicative layout with 28 – 30 puck positions arranged in a hexagonal pattern. The lid type is still undefined, but will be designed for efficient ice management. The Dewar will be realized in collaboration with a company specialized in cryogenic applications.
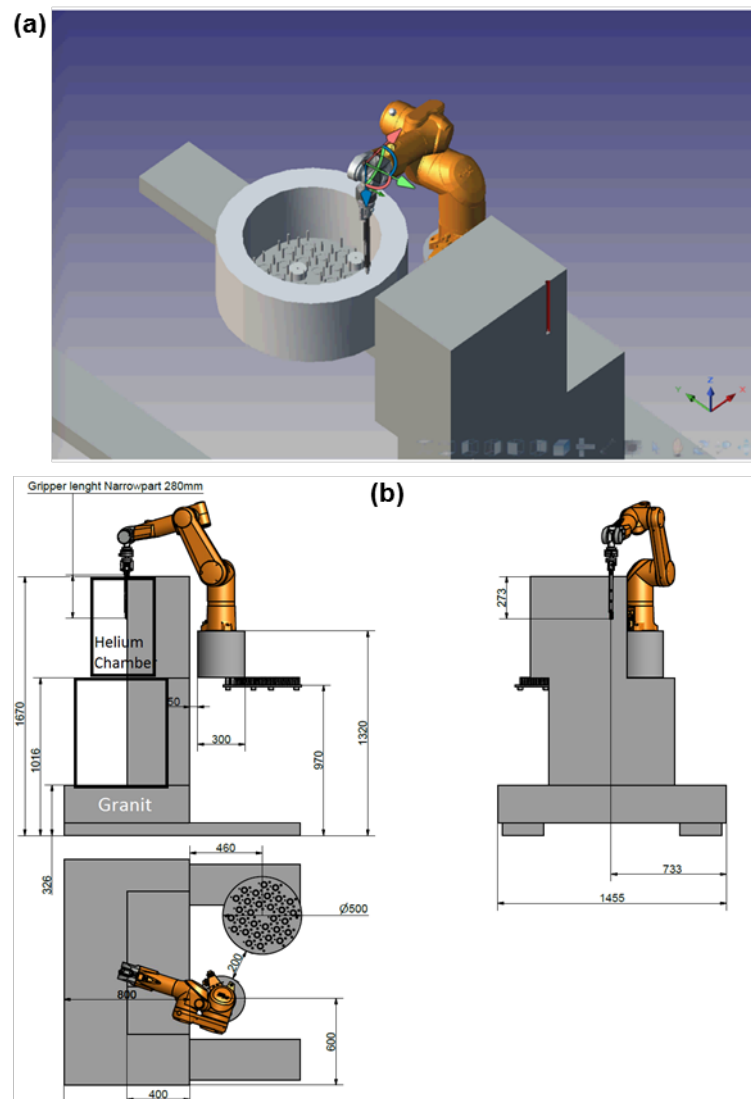
Figure 20. Concept of the sample changer unit.

Positioning of the sample changer unit components: Stäubli robot, Dewar base plate and Suna precision SG-1 gripper. (a) Three-dimensional view. The red cylinder represents the access path of the gripper through the chamber to the sample position. (b) Technical drawings in the three orthogonal projections.

5.4.3   Grippers

The gripper SG-1 from Suna precision GmbH (Figure 21) will be used as development platform, in a modified version to accommodate cryogenic chip mounting on the pin defined in section 5.2, adapted in length for compatibility with the ESB-MX chamber dimensions. This gripper includes a pneumatic crash protection and a mechanical collision sensor. A calibration tool and a room temperature gripper will also be developed.
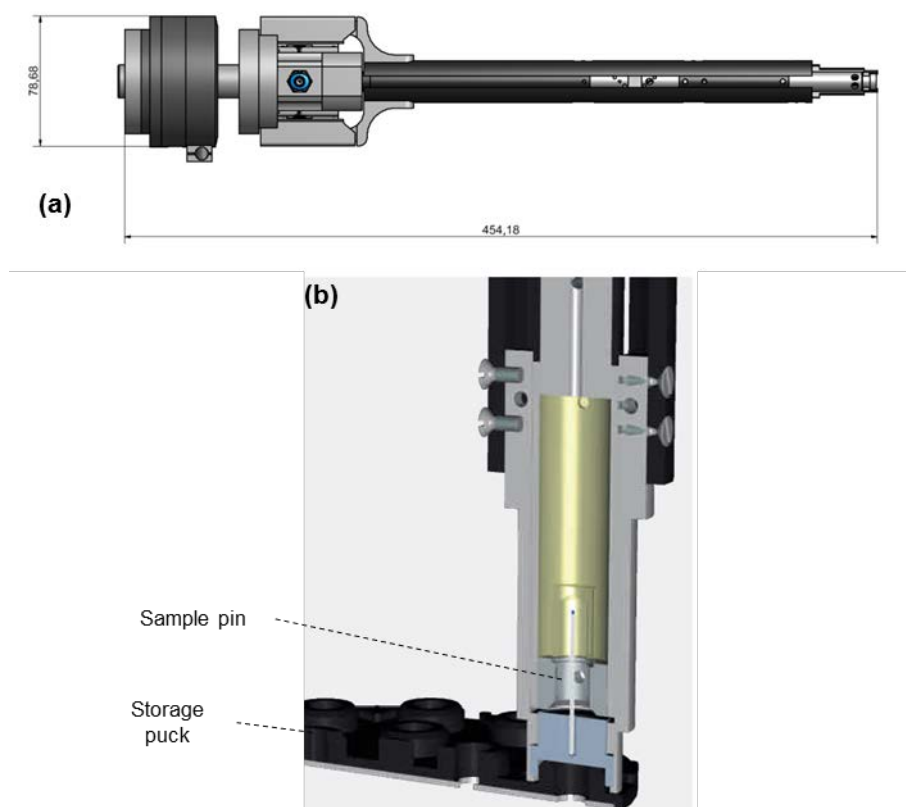
Figure 21. Sample changer gripper.

Gripper SG-1 from Suna precision (a), which grabs the sample pins from below (b). The inner diameter has been reduced from to 6.5 mm to 5.0 mm with respect to the original model, in order to hold chips of 5 x 5 mm size mounted on Spine pins or special ESB-MX pins.

5.4.4   Software

The software integration of the sample changer into the beamline environment is part of the sample changer project. This includes collision handling and recovery procedures, based on collision detection from the gripper and/or robot arm current.

5.4.5   Complementary equipment

The complementary equipment includes the robot stand, the gripper dryer and spare gripper stand, and the room temperature sample storage.

5.5   Electronics rack (WP5)

All control electronics for the ESB-MX instrument will be mounted in a moveable half-height 19" rack unit. These electronics components are the motor controllers, which include two DeltaTau PowerBrick, the cryo-jet controller, helium gas flow and pressure controllers, detector readout electronics, and the TTL signal generator. The camera servers are provided within the SwissFEL infrastructure. The electronics rack does not include the controller for the sample changer.

The connections from the ESB-MX rack to the ESB hutch infrastructure include electrical power, network connections, the SwissFEL timing signal (see section 5.6), and connections to the

camera servers for the two ESB-MX cameras. All connections from the ESB-MX rack to the ESB hutch and the ESB-MX instrument must allow rapid connection and disconnection.

5.6   Software and controls (WP6)

5.6.1   Overview ESB-MX control system

SwissFEL relies on an EPICS network for the control system, which is accessed by the user through a dedicated, python-based user interface. It also serves to program the various devices. The system will be exploited to control the ESB-MX instrument. SwissFEL also provides timing signals at 100 Hz for synchronization purposes ("SwissFEL timing system"), distributed over a separate network over the whole SwissFEL building.

From the control point of view, the instrument consists of two main units which are almost independent: the sample changer and the experimental chamber. Coordination to ensure that the sample changer gripper is not inside the chamber when X-rays are illuminating the sample will be achieved by logic signals indicating the states of the two units, and exchanged through TTL signal connections.

5.6.2   ESB-MX procedures and synchronization

The most relevant procedures to operate the ESB-MX instrument will be:

- Alignment of the experimental chamber to the X-ray beam path
- Sample mounting / dismounting
- Sample alignment without X-ray beam
- Sample alignment with X-ray beam (*)
- PX data acquisition (*)

The procedures labeled with an asterisk involve synchronization to the X-ray pulses. Any motion execution or signal detection will synchronized to the SwissFEL 100 Hz master clock. This is in contrast with the data acquisition procedures employed at synchrotron sources, where the beam is continuous on the timescales relevant to sample motion, and the sample motion itself represents the clock on which other operations are synchronized.

The SwissFEL timing system distributes a series of trigger signals at a 100 Hz repetition rate over a dedicated fiber network. Any beam synchronous procedure will rely on these signals. These can also be converted into logic TTL signals, specific to the user's demands, that are distributed over a TTL network and used to trigger motion sequences, to synchronize motion execution to the X-ray pulses, and to trigger the readout of detectors.

In addition to the trigger signals, the SwissFEL timing system distributes a pulse specific identification label ("pulse ID"). The readout signals of any detector equipped with an event receiver card are stamped with this label before they are broadcast to the data stream. This ensures at any time a reliable correlation at any later time of the data from different detectors that belong to the same FEL pulse.

5.6.3   Beam synchronous PX data acquisition

The fixed-target PX data acquisition with the ESB-MX instrument will be implemented in line with the concepts mentioned in the previous section. Figure 22 illustrates the devices involved in a typical data acquisition scan (see section 3.3). The diffractometer motions will be controlled by

a DeltaTau real-time motion control unit, which is the standard at SwissFEL, and allows smooth motion control synchronized to the 100 Hz master clock. Implementation of the motion control system will definitely be challenging for the fast scanning data acquisition mode at 100 Hz because of the required motion precision.
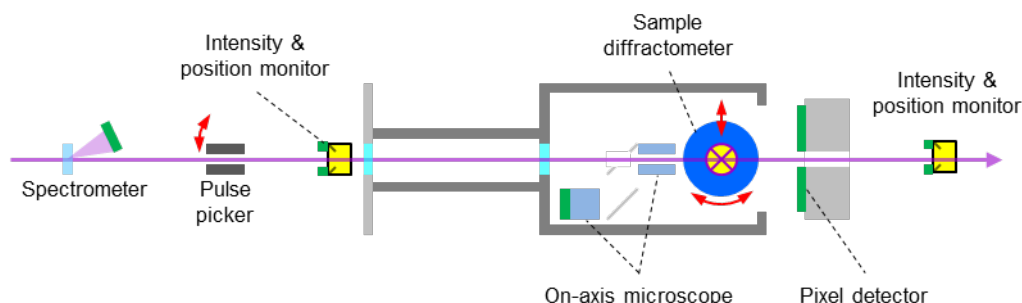
Figure 22. Devices involved in data acquisition.

Illustration of the devices involved in a fixed-target scan in air and at room temperature. The red arrows indicate motions that have to be synchronized with the X-ray beam. The detectors are in green and can be read out in beam synchronous manner.

5.6.4   Data collection workflow

Figure 23 displays the workflow of the PX measurement schemes supported by the ESB-MX instrument (section 3.3). The two data acquisition modes are conceptually the same. They differ in details of the sample position assessment and in the features of the motion to be implemented and executed.
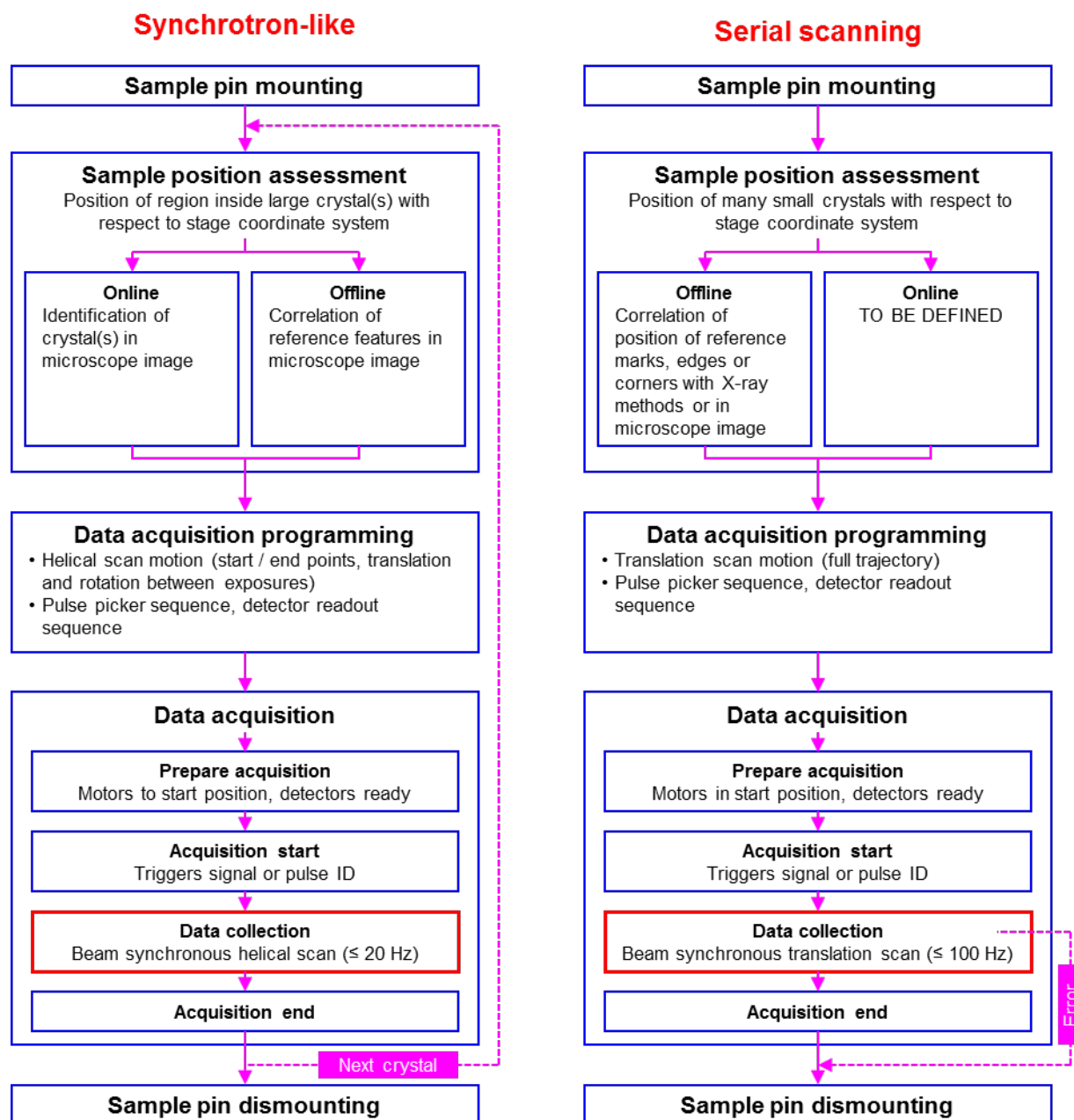
Figure 23. Data collection workflow.

Graphical illustration of the data collection workflow for synchrotron-like measurements (left) and scanning measurements (right). For the latter, online monitoring of the collected images (e.g. number of Bragg peak per image) will allow to interrupt a longer scan in case of insufficient data quality.

5.6.5   Data flow at SwissFEL

According to the SwissFEL IT infrastructure concept, data from a user-defined list of detectors belonging to the same FEL pulse ID will be stored in a single HDF5 container, to be available for analysis with a latency time of few seconds. These data include the Jungfrau detector images as well as camera images, beam intensities and positions, diode readouts, and fluorescence detector readouts. In addition, a data stream with latency time of less than a second will be

generated, which includes readouts of point or line detectors and scalars derived from 2D images from X-ray pixel array detectors and cameras such as peak centers, peak widths or number of peaks. These data will be available "instantaneously" to the user for monitoring the evolution of a measurement.

6 Possible upgrades

6.1 Pump-laser excitation in the visible range

The project objectives specify that the ESB-MX instrument has to be designed such that an upgrade to include the sample excitation with a pump laser is feasible with minor hardware modifications.

The pump-laser upgrade will aim for the following goals:

- Colinear in-coupling
- Wavength range 800 – 300 nm
- Focus at sample position, focus size < 40 μm FWHM
- Peak fluence at least 5 mJ/cm^2, if possible as high as 100 J/cm^2

The in-coupling will be achieved with a drilled parabolic mirror that focuses the parallel laser beam to the sample, such that downstream the laser beam propagates collinearly to the X-ray path. This solution will require a modification of the on-axis microscope to allow the transit of the wider laser beam through the objective. The concept shall be suitable for using the femtosecond laser infrastructure available at the SwissFEL experimental stations (in particular ESB) or any custom laser brought by the users that can be transported into the experimental hutch and integrated in the SwissFEL control system.

6.2 On-site room temperature sample preparation and humidified sample environment

The ESB-MX setup can be adapted to allow room temperature data collection with the protein crystal preserved by a humidifier during data collection, which can be mounted at the location of the cryo-jet nozzle. The protein crystal can be harvested and prepared on the sample pin either at an external laboratory and stored in a humidified container until data collection, or on-site in the experimental hutch just before the data collection is started.

7   Appendix

7.1   Jungfrau detector technology

The Jungfrau technology (TDR available at the SwissFEL homepage [36]) has been developed within the Detector group at PSI with the goal of realizing a pixel detector for the hard X-ray regime compatible with the femtosecond pulse durations of SwissFEL that maintains single photon resolution. The main features are reported in Table 7. The single module contains 0.5M pixels, but the modules can be easily combined in larger detection areas, such as the 16M detectors foreseen for the ESA and ESB stations at SwissFEL.

Parameter / Feature	Value / Description
Detection type	Charge integrating, three-stage gain, dynamic gain switching
Pixel size	75 μm
Dynamic range	> 10^4 (linearity better than 1%) @ 12 keV
Photon energy range	> 2 keV (@single photon sensitivity)
Noise	< Poisson limit
Repetition rate	< 2.4 kHz
Module size	1024 x 512 pixels, 8 x 4 cm

Table 7. Jungfrau detector features.

7.2   X-ray beam parameters

Table 8 and Table 9 show the X-ray beam parameters relevant for the operation at the ESB-MX instrument at the ESB station with in-air and in-helium setups.

Setup	E	T_{BI}	T_{EC}	T	3rd HC	N_{Sam}	3rd HC att.
Air	6.0 keV	0.50	0.28	0.14	<10^{-6}	$2.0 \cdot 10^{11}$	$1.1 \cdot 10^{-5}$
	8.0 keV	0.63	0.59	0.37		$4.0 \cdot 10^{11}$	<10^{-6}
	10.0 keV	0.54	0.76	0.41		$3.6 \cdot 10^{11}$	
	12.0 keV	0.56	0.85	0.48		$3.5 \cdot 10^{11}$	
Helium	5.0 keV	0.37	0.99	0.37	<10^{-6}	$6.5 \cdot 10^{11}$	$2.2 \cdot 10^{-4}$
	6.0 keV	0.50	0.99	0.50		$7.2 \cdot 10^{11}$	$3.3 \cdot 10^{-6}$
	8.0 keV	0.63	0.99	0.62		$6.8 \cdot 10^{11}$	<10^{-6}
	10.0 keV	0.54	1.00	0.54		$4.7 \cdot 10^{11}$	
	12.0 keV	0.56	1.00	0.56		$4.1 \cdot 10^{11}$	

Table 8. X-ray beam parameters at the ESB-MX sample position.

The parameters are given for both in-air and in-helium setups at various photon energies, and include the transmission of the ESB beamline (T_{BI}), the transmission in the ESB-MX experimental chamber (T_{EC}), the total transmission (T) and the third-harmonic contamination (3rd HC) at the sample position, and the number of photons at the sample position (N_{Sam}) assuming an incoming FEL pulse of 1.4 mJ energy. The last column shows the third harmonic contamination for the beam attenuated by a factor of 100 by inserting Si attenuators.

The beamline elements include 2 offset mirrors and 2 KB focusing mirrors (ARAMIS CDR available at the SwissFEL homepage [36]), followed by a 100 μm thick diamond window.

For in-air operation, the beam propagation path was assumed to be through 1000 mm in 10^{-3} mbar vacuum, through a 50 μm diamond window and through 400 mm in atmospheric air.

For in-helium operation, the beam propagation path was assumed to be through 1400 m in helium at ambient pressure.

Setup	E	T_{Fwd}	$T_{FWD}(3^{rd})/T_{FWD}$	T_{60^o}	$T_{60^o}(3^{rd})/T_{60^o}$
Air	6.0 keV	0.76	1.30	0.58	1.69
	8.0 keV	0.89	1.10	0.80	1.24
	10.0 keV	0.95	1.05	0.89	1.11
	12.0 keV	0.97	1.03	0.94	1.07
Helium	5.0 keV	0.65	1.51	0.39	2.50
	6.0 keV	0.78	1.26	0.58	1.68
	8.0 keV	0.90	1.10	0.80	1.23
	10.0 keV	0.95	1.05	0.89	1.11
	12.0 keV	0.97	1.03	0.94	1.06

Table 9. Diffraction signal transmission.

The transmissivity of the signal diffracted from the sample to the detector in the forward and at 60º deflection (T_{FWD} and T_{60^o}) is given for both in-air and in-helium setups at various photon energies. The third harmonic enhancements are also given ($T(3^{rd})/T$). For the in-air setup, the propagation is assumed in air with the detector at 100 mm from the sample. For the in-helium setup, the detector is assumed at 125 mm from the sample, with 119 mm and 6 mm propagation in helium (inside the chamber) and air (between chamber exit window and detector), respectively, and with 110 μm Kapton layer on the path.

7.3   Timeplan

The timeplan of the ESB-MX project is represented in Figure 24, and the project milestone are listed in Table 10. The ESB-MX instrument is planned to be ready for commissioning at the SwissFEL ESB experimental station in Mai 2018, and two 5 – 6 day commissioning periods are foreseen in the following 6 – 10 months. The full instrument with the exception of the sample changer unit will be pre-commissioned with beam at the X06SA PX beamline at the SLS during two 5 – 6 day commissioning periods.
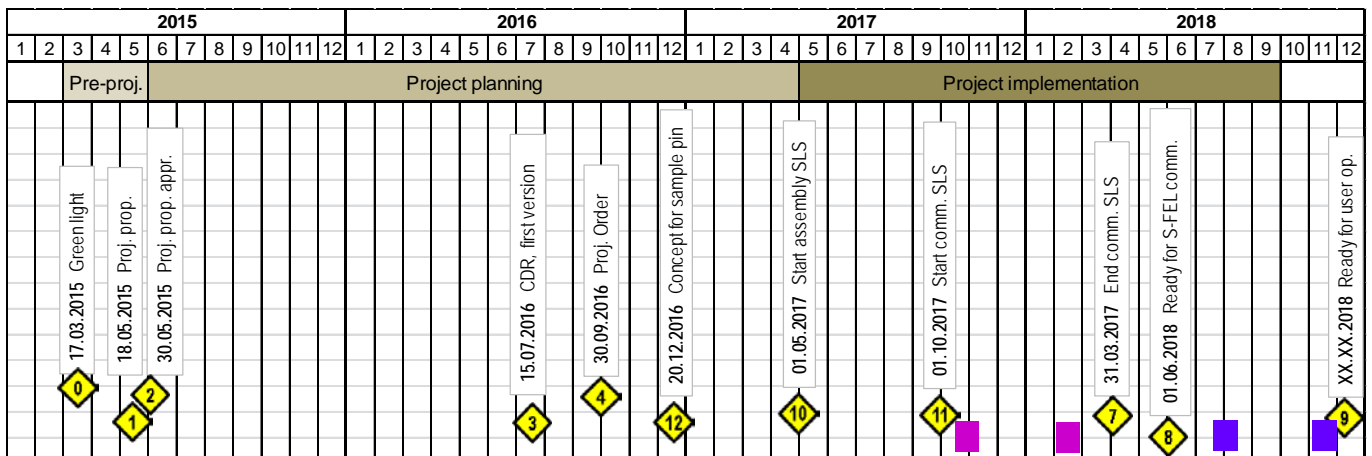
Figure 24. ESB-MX project timeplan.

The timeplan includes the project milestones, the two commissioning campaigns at the SwissFEL ESB station (violet rectangles, exact date unknown), as well as the two pre-commissioning campaigns at the SLS X06SA beamline (magenta rectangles, dates fixed after SLS shutdowns).
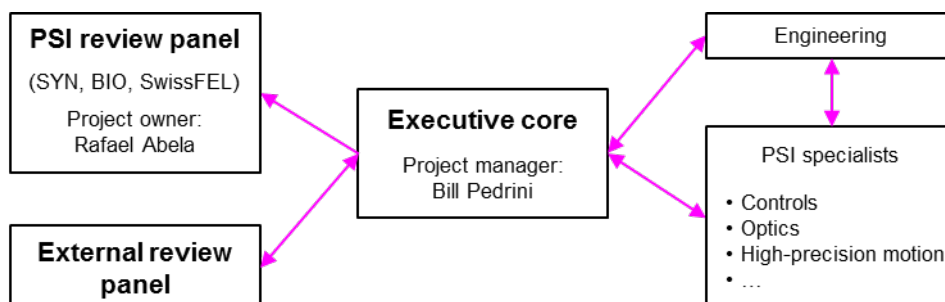
	Milestone	Remarks	Due date
0	Green light for project start		17.03.2015
1	Project proposal	Project objectives and budget	18.05.2015
2	Project proposal approved		30.05.2015
3	Concept design report, first draft	Revised project objectives and budget, concept for the instrument, main technical challenges identified and solution established	15.07.2016
4	Project order	Green light for project continuation with revised objectives and budget	30.09.2016
12	Concept for sample pin	Prototype of sample pin and sample pin holder is tested	20.12.2016
10	Start assembly at SLS	Start assembly of the experimental chamber in dedicated laboratory space	01.05.2017
11	Start commissioning at SLS	Experimental chamber is ready to be commissioned with beam at the SLS X06SA beamline	01.10.2016
7	End commissioning at SLS	All ESB-MX devices ready to be transported at SwissFEL	31.03.2017
8	Ready for SwissFEL commissioning	All ESB-MX devices ready to be installed at the ESB station for allocated beamtime	01.06.2018
9	Ready for user operation	Commissioning in air and in helium finished	na

Table 10. ESB-MX project milestones.

The milestone numbering doest not reflect their temporal ordering. Milestones with dates shadowed in green have been achieved.

7.4   Project organization

The ESB-MX project organization is represented in Figure 25. The executive core of the project is responsible for the design, the realization and the commissioning of the ESB-MX instrument, with the responsibles of the six workpackages listed in Table 11. Engineering is ensured by a full-time person at PSI. Support for various technical aspects (controls, optics, high-precision motions, …) is provided by PSI internal staff. The executive core reports about twice a year on the achieved progress to the PSI internal review panel, which includes representatives from the SYN and BIO divisions as well as from the SwissFEL project organization. An external review panel will revise the CDR.

Figure 25. ESB-MX project organization.

	Workpackage	Tasks	Responsible
WP1	Experimental chamber	• Conceive and design the experimental chamber, including chamber support and cryo jet • Procure / Coordinate fabrication of chamber components • Coordinate assembly of experimental chamber, sample diffractometer and sample pin holder	Bill Pedrini (SwissFEL)
WP2	Sample diffractometer	• Evaluate solutions for the sample diffractometer that fulfill the project specifications • Procure the hardware components for the sample diffractometer	Claude Pradervand (SwissFEL)
WP3	Pin and pin holder	• Conceive, design and test a system including the sample pin and the sample pin holder which is compatible with the automated sample changer and which fulfils the sample motion specifications, and which is compatible with integration of standard fixed target sample mount systems used at synchrotron sources • Ensure the availability of (at least) one solution for a sample chip that can be used to fulfil the sample motion specifications	Isabelle Martiel (SYN)
WP4	Sample changer	• Coordination with the sample changer project at the SLS-MX group • Ensure implementation of special requirements for the ESB-MX sample changer unit	Isabelle Martiel (SYN)
WP5	Electronic rack	• Define, procure and build all the electronics infrastructure necessary to control the ESB-MX instrument (except that related to the sample changer unit) • Coordinate integration of electronics with the ESB infrastructure	Claude Pradervand (SwissFEL)
WP6	Software and controls	• Ensure integration of electronic hardware within the SwissFEL control system • Develop the ESB-MX data acquisition interface, and ensure its integration in the SwissFEL data acquisition system • Program / Ensure programming of complex motions	Ezequiel Panepucci (SYN)

Table 11. ESB-MX project workpackages.

Tasks and responsibles of the six ESB-MX workpackages. PSI affiliations: SYN = SYN Division; SwissFEL = SwissFEL Project.

7.5   Glossary

PSI   Paul Scherrer Institute

SLS   Swiss Light Source

MX   Macromolecular crystallography group

PX   Protein Crystallography

SwissFEL   Swiss X-ray free electron laser

ARAMIS   Hard X-ray beamline at SwissFEL

ESA/B/C   Hard X-ray experimental stations at SwissFEL

References

1. Schlichting, I., *Serial femtosecond crystallography: the first five years.* IUCrJ, 2015. **2**(2): p. 246-55.

2. Neutze, R., et al., *Potential for biomolecular imaging with femtosecond X-ray pulses.* Nature, 2000. **406**(6797): p. 752-7.

3. Chapman, H.N., et al., *Femtosecond X-ray protein nanocrystallography.* Nature, 2011. **470**(7332): p. 73-7.

4. Huang, C.Y., et al., *In meso in situ serial X-ray crystallography of soluble and membrane proteins.* Acta Crystallogr D Biol Crystallogr, 2015. **71**(6): p. 1238-56.

5. Tenboer, J., et al., *Time-resolved serial crystallography captures high-resolution intermediates of photoactive yellow protein.* Science, 2014. **346**(6214): p. 1242-6.

6. Kern, J., et al., *Taking snapshots of photosynthetic water oxidation using femtosecond X-ray diffraction and spectroscopy.* Nat Commun, 2014. **5**: p. 4371.

7. Liu, W., et al., *Serial femtosecond crystallography of G protein-coupled receptors.* Science, 2013. **342**(6165): p. 1521-4.

8. Kupitz, C., et al., *Serial time-resolved crystallography of photosystem II using a femtosecond X-ray laser.* Nature, 2014. **513**(7517): p. 261-5.

9. Hunter, M.S., et al., *Fixed-target protein serial microcrystallography with an x-ray free electron laser.* Sci Rep, 2014. **4**: p. 6026.

10. Cohen, A.E., et al., *Goniometer-based femtosecond crystallography with X-ray free electron lasers.* Proceedings of the National Academy of Sciences, 2014. **111**(48): p. 17122-17127.

11. Hirata, K., et al., *Determination of damage-free crystal structure of an X-ray-sensitive protein using an XFEL.* Nat Methods, 2014. **11**(7): p. 734-6.

12. Lyubimov, A.Y., et al., *Capture and X-ray diffraction studies of protein microcrystals in a microfluidic trap array.* Acta Crystallogr D Biol Crystallogr, 2015. **71**(4): p. 928-40.

13. Frank, M., et al., *Femtosecond X-ray diffraction from two-dimensional protein crystals.* IUCrJ, 2014. **1**(2): p. 95-100.

14. Roedig, P., et al., *A micro-patterned silicon chip as sample holder for macromolecular crystallography experiments with minimal background scattering.* Sci Rep, 2015. **5**: p. 10451.

15. Pedrini, B., et al., *7 A resolution in protein two-dimensional-crystal X-ray diffraction at Linac Coherent Light Source.* Philos Trans R Soc Lond B Biol Sci, 2014. **369**(1647): p. 20130500.

16. Gati, C., et al., *Serial crystallography on in vivo grown microcrystals using synchrotron radiation.* IUCrJ, 2014. **1**(2): p. 87-94.

17. Calero, G., et al., *Identifying, studying and making good use of macromolecular crystals.* Acta Crystallogr F Struct Biol Commun, 2014. **70**(8): p. 993-1008.

18.   Emma, P., et al., *First lasing and operation of an ångstrom-wavelength free-electron laser.* Nature Photonics, 2010. **4**(9): p. 641-647.

19.   Sierra, R.G., et al., *Concentric-flow electrokinetic injector enables serial crystallography of ribosome and photosystem II.* Nat Methods, 2016. **13**(1): p. 59-62.

20.   Boutet, S. and G.J. Williams, *The Coherent X-ray Imaging (CXI) instrument at the Linac Coherent Light Source (LCLS).* New Journal of Physics, 2010. **12**(3): p. 035024.

21.   Sherrell, D.A., et al., *A modular and compact portable mini-endstation for high-precision, high-speed fixed target serial crystallography at FEL and synchrotron sources.* J Synchrotron Radiat, 2015. **22**(6): p. 1372-8.

22.   Boutet, S., A.E. Cohen, and S. Wakatsuki, *The New Macromolecular Femtosecond Crystallography (MFX) Instrument at LCLS.* Synchrotron Radiation News, 2016. **29**(1): p. 23-28.

23.   https://portal.slac.stanford.edu/sites/lcls_public/lcls_ii/Pages/default.aspx.

24.   Yabashi, M., H. Tanaka, and T. Ishikawa, *Overview of the SACLA facility.* J Synchrotron Radiat, 2015. **22**(3): p. 477-84.

25.   Tono, K., et al., *Beamline, experimental stations and photon beam diagnostics for the hard x-ray free electron laser of SACLA.* New Journal of Physics, 2013. **15**(8): p. 083035.

26.   Tono, K., et al., *Diverse application platform for hard X-ray diffraction in SACLA (DAPHNIS): application to serial protein crystallography using an X-ray free-electron laser.* J Synchrotron Radiat, 2015. **22**(3): p. 532-7.

27.   Song, C., et al., *Multiple application X-ray imaging chamber for single-shot diffraction experiments with femtosecond X-ray laser pulses.* Journal of Applied Crystallography, 2014. **47**(1): p. 188-197.

28.   Abela, R., et al., *XFEL: The European X-Ray Free-Electron Laser - Technical Design Report.* 2006, Hamburg: DESY.

29.   Mancuso, A.P. *Conceptual Design Report: Scientific Instrument Single Particles, Clusters, and Biomolecules (SPB).* 2011. DOI: DOI:10.3204/XFEL.EU/TR-2011-007.

30.   Mancuso, A.P., et al. *Technical Design Report: Scientific Instrument Single Particles, Clusters, and Biomolecules (SPB).* XFEL.EU Technical Report, 2013. 1-232 DOI: DOI:10.3204/XFEL.EU/TR-2013-004.

31.   Bressler, C. *Conceptual Design Report: Scientific Instrument FXE.* 2011. DOI: DOI:10.3204/XFEL.EU/TR-2011-005.

32.   Bressler, C., A. Galler, and W. Gawelda *Technical Design Report: Scientific Instrument FXE.* 2012. DOI: DOI:10.3204/XFEL.EU/TR-2012-008.

33.   Park, J., et al., *Design of a hard X-ray beamline and end-station for pump and probe experiments at Pohang Accelerator Laboratory X-ray Free Electron Laser facility.* Nuclear Instruments and Methods in Physics Research Section A: Accelerators, Spectrometers, Detectors and Associated Equipment, 2016. **810**: p. 74-79.

34.   Patterson, B.D., et al., *Coherent science at the SwissFEL x-ray laser.* New Journal of Physics, 2010. **12**(3): p. 035012.

35.   Tschentscher, T. *Layout of the X-Ray Systems at the European XFEL.* 2011. DOI: DOI:10.3204/XFEL.EU/TR-2011-001.

36.   *https://www.psi.ch/swissfel/swissfel*.

37.   *https://embl.fr/newpin*.